



HAL
open science

Low energy theory of the t - t' - t'' - U Hubbard Model at half-filling: interaction strengths in cuprate superconductors and an effective spin-only description of La_2CuO_4 .

Jean-Yves Delannoy, M. J. P. Gingras, Peter C.W. Holdsworth, A.-M. S. Tremblay

► **To cite this version:**

Jean-Yves Delannoy, M. J. P. Gingras, Peter C.W. Holdsworth, A.-M. S. Tremblay. Low energy theory of the t - t' - t'' - U Hubbard Model at half-filling: interaction strengths in cuprate superconductors and an effective spin-only description of La_2CuO_4 . 2008. hal-00311789

HAL Id: hal-00311789

<https://hal.science/hal-00311789v1>

Preprint submitted on 22 Aug 2008

HAL is a multi-disciplinary open access archive for the deposit and dissemination of scientific research documents, whether they are published or not. The documents may come from teaching and research institutions in France or abroad, or from public or private research centers.

L'archive ouverte pluridisciplinaire **HAL**, est destinée au dépôt et à la diffusion de documents scientifiques de niveau recherche, publiés ou non, émanant des établissements d'enseignement et de recherche français ou étrangers, des laboratoires publics ou privés.

Low energy theory of the $t - t' - t'' - U$ Hubbard Model at half-filling: interaction strengths in cuprate superconductors and an effective spin-only description of La_2CuO_4 .

J.-Y. P. Delannoy,^{1,2} M. J. P. Gingras,^{2,3} P. C. W. Holdsworth,¹ and A.-M. S. Tremblay⁴

¹*Université de Lyon, Laboratoire de Physique, CNRS,*

École normale supérieure de Lyon, 46 Allée d'Italie, 69364 Lyon cedex 07, France.

²*Department of Physics and Astronomy, University of Waterloo, Ontario, N2L 3G1, Canada*

³*Department of Physics and Astronomy, University of Canterbury, Private Bag 4800, Christchurch, New Zealand*

⁴*Département de Physique and RQMP, Université de Sherbrooke, Sherbrooke, Québec, J1K 2R1, Canada.*

(Dated: August 22, 2008)

Spin-only descriptions of the half-filled one-band Hubbard model are relevant for a wide range of Mott insulators. In addition to the usual Heisenberg exchange, many new types of interactions, including ring exchange, appear in the effective Hamiltonian in the intermediate coupling regime. In order to improve on the quantitative description of magnetic excitations in the insulating antiferromagnetic phase of copper-oxide (cuprate) materials, and to be consistent with band structure calculations and photoemission experiments on these systems, we include second and third neighbor hopping parameters, t' and t'' , into the Hubbard Hamiltonian. A unitary transformation method is used to find systematically the effective Hamiltonian and any operator in the spin-only representation. The results include all closed, four hop electronic pathways in the canonical transformation. The method generates many ring exchange terms that play an important role in the comparison with experiments on La_2CuO_4 . Performing a spin wave analysis, we calculate the magnon dispersion as a function of U, t, t' and t'' . The four parameters are estimated by fitting the magnon dispersion to the experimental results of Coldea *et al.* [Phys. Rev. Lett. **86**, 5377, 2001] for La_2CuO_4 . The ring exchange terms are found essential, in particular to determine the relative sign of t' and t'' , with the values found in good agreement with independent theoretical and experimental estimates for other members of the cuprate family. The zero temperature sublattice magnetization is calculated using these parameters and also found to be in good agreement with the experimental value estimated by Lee *et al.* [Phys. Rev. B **60**, 3643 (1999)]. We find a value of the interaction strength $U \simeq 8t$ consistent with Mott insulating behavior.

I. INTRODUCTION

High temperature superconductors have challenged almost every traditional concept and method of condensed matter theory. Ill understood issues concerning Fermi liquids and quantum critical behavior for example, may be intimately related to the problem of superconductivity itself. From the very beginning, it has therefore appeared important to develop a better understanding of quantum magnetism in general, given that the parent compounds of high-temperature superconductors are insulating antiferromagnets. For example, although these compounds are Néel ordered, it was proposed early on that, in two dimensions, the ground state of the Heisenberg antiferromagnet might be very close to being a resonating-valence bond state rather than a Néel ordered state¹. This turns out not to be true, but it took some time to establish numerically that the ground state is indeed ordered^{2,3}, in agreement with experiment^{4,5}.

Issues relating to the quantum magnetism of the copper-oxide materials (cuprates) have resurfaced in the last few years. Detailed neutron scattering experiments on the parent high-temperature superconductor La_2CuO_4 illustrate that the question of which model best describes these compounds⁶ can now be addressed with precision. For example, while the magnetic properties of Copper Deuterioformate Tetradeuterate can be described

in detail using the Heisenberg model⁷, La_2CuO_4 exhibits clear deviations⁶ from it.

Specifically, the observed spin wave dispersion along the antiferromagnetic Brillouin zone boundary is not predicted by the Heisenberg model. One can in principle account for these differences by introducing phenomenological two-spin and multi-spin exchange constants into the spin Hamiltonian. These spin Hamiltonians can be deduced, as shown by Dirac^{8,9,10}, from general considerations of symmetry and permutation operators and the value of the exchange constants can be fixed by fitting to the experimental data. However, in our opinion, a more interesting approach is that taken by Coldea *et al.*⁶. The authors of Ref. [6] take the point of view, which we share, that the one-band Hubbard model is a more fundamental starting point for the description of the copper oxygen planes in these materials if one wants to connect the magnetism at the microscopic level with electronic correlation effects. Although in this paper we concentrate on half filling, it may also be valid on moving away from half-filling, into the region where the fermions eventually pair to give high-temperature superconductivity.

The one band Hubbard Hamiltonian H_{H} is one of the simplest lattice models of interacting electron that admits a “rich” phenomenology resembling that of the cuprates. A key feature of this model is that it does describe both the insulating and metallic phases and the

(Mott) transition between them. In interaction-induced insulators, the band is half-filled and insulating behavior occurs because of interactions, not because of band folding induced by long-range order. However, in two-dimensions a half-filled band can be insulating because of a pseudogap induced by fluctuating antiferromagnetism, or because of the Mott phenomenon. In the former case (weak coupling), the pseudogap appears when the thermal de Broglie wavelength ξ_{th} is less than the antiferromagnetic correlation length¹¹ ξ , while in the latter Mott insulating case (strong coupling), the system is insulating even when this condition is not satisfied. In La_2CuO_4 neutron measurements have been done only in the regime where $\xi > \xi_{\text{th}}$, so that antiferromagnetic correlations could be the source of the insulating behavior. In a very recent paper¹² Comanac *et al.* used *single-site* dynamical mean-field theory (DMFT) to calculate the optical conductivity of La_2CuO_4 . The authors of Ref. [12] found that La_2CuO_4 , or at least its optical conductivity, is best parametrized by a U/t smaller than that necessary for the Mott transition in single-site DMFT. Consequently, the authors of Ref. [12] argue that correlations in the cuprates may not be as strong as generally believed and that these materials may not be Mott insulators but rather, that the development of antiferromagnetism is necessary to drive the insulating state. On the other hand, *cluster*-DMFT calculations, which are more accurate in two dimensions, find that the inclusion of short-range antiferromagnetic correlations, which is possible in *multi-site* calculations, reduce considerably the critical $(U/t)_{\text{Mott}}$ necessary for the Mott transition compared with single-site DMFT^{13,14,15,16}.

This leads to one of the key questions in this field. Do the strange properties observed in underdoped cuprates at finite temperature arise from interaction-induced localisation (Mott insulator) or from competing phases? If interactions are not strong enough to lead to a Mott insulator, competing phases arising at weak coupling are the only remaining possibility.

To find parameters appropriate for high-temperature superconductors, Coldea *et al.* used earlier theoretical results^{17,18} relating the parameters of the Hubbard model, hopping energy t and on-site interaction U , to the exchange constants in an effective spin-Hamiltonian. The parameters in the Hubbard model were deduced by fitting the resulting effective low-energy spin theory to the spin-wave dispersion relation. This is quite a remarkable result. Indeed, had the Heisenberg limit accurately described the Hubbard model, only the value of t^2/U could have been deduced from neutron experiments. The appearance of corrections to the Heisenberg model to higher order in powers of t/U allows one to obtain t and U separately, the former being an effective electronic band quantity.

However, to be consistent with a general message provided by Angle Resolved Photoemission Spectroscopy (ARPES)^{19,20,21,22} experiments, optical experiments²³ and with results from band structure calculations^{24,25} on

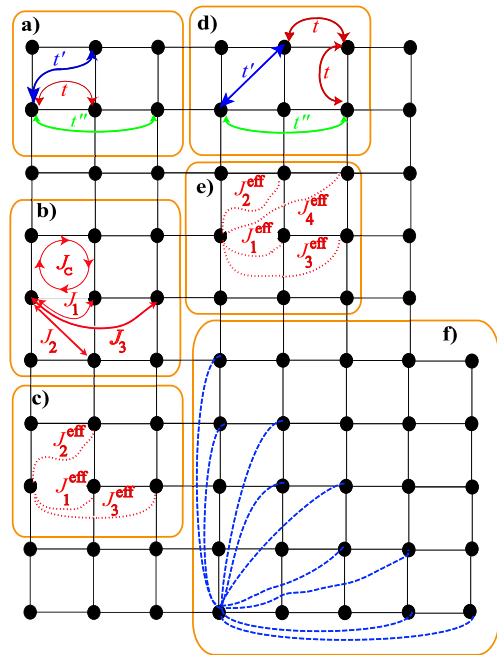


FIG. 1: (Color online) Hopping processes and resulting spin interactions. **a)** shows the different hopping processes characterized by parameters t , t' and t'' in the Hubbard model considered in this paper. t , t' and t'' are hopping parameters between first, second and third nearest neighbors, respectively. **b)** At half-filling, and when $t' = t'' = 0$, canonical perturbation theory leads to order t^4/U^3 to an effective spin-1/2 Hamiltonian, $H_s^{(4)}$, characterized by first (J_1), second (J_2) and third (J_3) nearest neighbor exchange interactions as well as a 4-spin ring (cyclic) exchange interaction with coupling strength J_c . **c)** In a large S expansion, $H_s^{(4)}$ can be recast to order $1/S$ as an effective spin Hamiltonian which only involves bilinear (pairwise) spin-spin exchange interactions between first (J_1^{eff}), second (J_2^{eff}) and third (J_3^{eff}) nearest neighbors. To order $1/S$, the effect of the ring exchange of strength J_c merely renormalizes the first and second nearest-neighbor exchange as discussed in Ref. [6]. **d)** illustrates an example of a four hops (ring exchange) electronic process that involves t' and t'' and contribute to order $t^2 t' t'' / U^3$ to the spin Hamiltonian $H_s^{(4)}$. **e)** shows that the ring exchange term illustrated in **d)** introduces in the $1/S$ approximation of $H_s^{(\text{eff})}$ a fourth nearest neighbor exchange, J_4^{eff} as well as renormalize the J_1^{eff} , J_2^{eff} and J_3^{eff} of **c)**. **f)** illustrates all the additional J_n^{eff} exchanges beyond those shown in **c)** and which are generated by all the hopping processes involving an allowed combination of t , t' and t'' to order $1/U^3$.

a wide variety of quasi two-dimensional cuprate materials, it is necessary to include in the Hubbard model both second (t') and third (t'') nearest-neighbor hopping, as they have been found to have sizable values in all the above studies (see Fig. 1). In this paper we thus address the following questions: What is the effect of these additional hopping constants on the magnetic properties of the cuprates, and on La_2CuO_4 in particular? Can their “effective” values and that of U within the Néel or-

der phase be determined by comparing experimental spin wave dispersion data with theoretical calculations?

As a first step to address the question of the strength of t , t' , t'' and U in La_2CuO_4 , we incorporate the effects of these extra hopping constants into a one-band Hubbard model from which we derive an effective spin-only Hamiltonian description of La_2CuO_4 . As we shall see, the effects of t' and t'' are rather subtle and can even sometimes compensate each other. It is only when these hopping terms have been included in the derivation of the effective spin Hamiltonian, with all the subsequent new ring exchanges, that one can extract more meaningful values of $t - t' - t'' - U$ from comparisons of theory with inelastic neutron scattering experiments. In particular, the values of t and U obtained by Coldea *et al.*⁶ place the underlying Hubbard model in the intermediate coupling regime where the band width and interaction energies are comparable and hence in the regime where one might expect an insulator to metal transition. Our more detailed analysis leads to a larger values of U , repositioning material relevant model parameters more clearly within the Mott insulating regime, as we will discuss more thoroughly at the end of this paper.

Although we analyze experiments on La_2CuO_4 , providing a specific materials context to our study, we believe that the parameters of the one-band Hubbard model that we extract below should be characteristic of the two-dimensional copper-oxygen planes of cuprate superconductors in general: specifically, band structure calculations do reveal variations of band parameters from one compound to the next^{25,26}, but overall, the band structure of CuO_2 planes is quite similar from one compound to the next²⁷. Even away from half filling, whether for hole or electron doped materials, the one-band Hubbard model for CuO_2 planes seems to contain much of the Physics of high-temperature superconductors^{28,29}. Our calculations should therefore have wider ranging applications than the detailed comparison with experiments on pure La_2CuO_4 presented below.

In the next two subsections of this Introduction, we describe in more detail the central issues and key results of this paper. There are two main parts to our work. In the first part, Section II, we derive the effective Hamiltonian to order $1/U^3$, including $t - t' - t''$. This derivation is exact and completely general. In the second part, Section III, we determine the spin wave energies, taking into account the quantum correction to the classical frequencies through the spin wave velocity renormalization factor, $Z_c(\mathbf{k})$, to lowest order in $1/S$. We then determine a parameter set $\{t, t', t'', U\}$ by fitting the experimental magnon excitation spectrum of Ref. [6]. The resulting set is in good agreement with values from ARPES experiments and band structure calculations on various cuprates. Further, we calculate the zero temperature staggered magnetization order parameter using the set $\{t, t', t'', U\}$ and compare it with experimental values. A more complete solution of the spin dynamics for the effective spin Hamiltonian derived herein, including magnon-

magnon interactions, would most likely require the use of numerical techniques³⁰, since it would be an arduous task to include in the self-energy corrections the multitude of magnon creation and annihilation terms present beyond the non-interacting approximation.

A. Spin-only description of Hubbard model and La_2CuO_4

In many strongly correlated quantum mechanical systems, the separation of energy scales allows the development of a low energy effective theory, through the integration over the high energy degrees of freedom. In this context, spin-only descriptions of strongly-correlated electron systems are an excellent example. Here, in the limit of strong electron-electron interaction, elimination of the states with one or more doubly occupied sites reduces exponentially the dimension of the relevant low energy Hilbert space, facilitating the theoretical and numerical description of the problem. Through this procedure, the regime of particular interest, where energy scales actually compete, can be approached perturbatively, via the introduction of a small parameter, the ratio of the kinetic to potential energy scales. However, the price one pays for this dimensional reduction is the generation of longer range and many particle interactions, as one moves into this intermediate regime. The derivation of such a theory can be achieved using different methods, leading to distinct expressions for the effective Hamiltonian, which can be shown to be equivalent through the application of a unitary transformation³¹. One of these methods, the canonical transformation (CT)^{18,32,33}, which we adopt below, is a convenient and systematic way of expanding a model like the Hubbard model to any order in the perturbation parameter.

In the regime where t/U remains a small parameter suitable for a perturbation theory, but where one moves away from the strictly Heisenberg limit ($t/U \rightarrow 0$), the pairwise exchange interactions are joined by ring, or cyclic exchange terms that couple more than 2 spins¹⁸. Large enough ring exchange terms have been found to drive some model systems into exotic, intrinsically quantum mechanical ground states^{34,35,36}. Indeed, there is currently a rapidly growing interest in the study of effective many-body non pairwise spin-spin interactions which lead to non-trivially correlated states in quantum spin systems^{37,38}.

In most theoretical work, the effort has so far focused on models with only the nearest-neighbor Heisenberg exchange and ring exchange. However, when starting from a microscopic fermionic Hamiltonian the strength of the ring exchange coupling is determined from the small parameter t/U and is not a free parameter, nor is it the sole higher order term arising in the resulting spin only theory. To the same order in perturbation, $t(t/U)^3$, the canonical transformation also generates second, J_2 , and third, J_3 , neighbor spin-spin interactions through pro-

cesses involving four electronic hops. The ring exchange, J_c , is thus only one of a set of spin interactions generated to this order^{18,31,33} and all should be taken into account. We remark that in the general approach of Dirac^{8,9}, the coupling constants multiply spin permutation operators, rather than spin operators themselves and thus have a different definition from those here. One finds that permutation of four spins lead to both four spin ring exchange terms and pure two-spin exchange when written in terms of spin operators¹⁰.

Within the $t-U$ Hubbard model, the inclusion of virtual hopping pathways of n hops thus introduces further neighbor spin couplings of order $t(t/U)^{n-1}$. For a compound with a band structure characterized by several tight-binding parameters of comparable value, one should consider the role of direct further neighbor hops over length scales comparable with the nearest neighbor pathways of length n , as well as the multiple hop terms. Hence, to develop a theory accurate to order $(1/U)^3$ one should include direct hopping to first, second and third nearest neighbors, characterized by energy scales t , t' and t'' , respectively. These hopping processes generate second and third neighbor Heisenberg exchange terms that compete with those generated by the four hop processes discussed above. There is evidence that this is the situation for the CuO_2 planes of parent superconducting materials: for example, in $\text{Sr}_2\text{CuO}_2\text{Cl}_2$, which has a half filled band, the hopping constants t' and t'' are estimated to be $t'/t \sim -0.3$, $t''/t \sim 0.2$, from comparisons of exact diagonalization with photoemission experiments³⁹. Very similar values are found from comparisons with other types of calculations⁴⁰ and from band structure calculations for $\text{YBa}_2\text{CuO}_3\text{O}_7$ ⁴¹. In fact these values are typical for insulating materials with copper-oxygen planes, including both hole and electron doped cuprates^{27,42}. For La_2CuO_4 , band structure calculations^{24,25} suggest smaller values of t'/t and t''/t . ARPES experiments are not available for this compound but they are for the doped system $\text{La}_{2-x}\text{Sr}_x\text{CuO}_4$ that becomes a high temperature superconductor. According to these experiments^{19,20,21,22}, t'/t and t''/t deduced from the shape of the Fermi surface are close to band structure values, although they are larger by about 30% for very lightly doped compound¹⁹. We will return to this issue later.

Given this range of values for t' and t'' one could expect the resulting exchange terms of order $t'(t'/U)$ or $t''(t''/U)$ to be of similar magnitude to those of order $t(t/U)^3$. This is one of the motivations for the work presented in this paper where we introduce all terms in a spin-only Hamiltonian that depend on t , t' and t'' and that are generated up to order $1/U^3$. We assess their importance, making particular reference to the magnetic properties of La_2CuO_4 . We show that the canonical transformation method^{18,31,33} can be easily generalized for the $t-t'-t''-U$ Hubbard model, giving a complete spin-only description for arbitrary first, second and third neighbor hopping, correct to order $1/U^3$.

B. Spin-wave analysis and comparison with experiment.

It has been known for some time that a spin wave analysis of the spin 1/2 Heisenberg antiferromagnet on a square lattice, taken to leading order in $1/S$, reproduces the zero point quantum fluctuations of the staggered moment to a good approximation⁴³. This is because the second order terms renormalize the classical magnon frequencies but do not induce magnon-magnon interactions and make zero contribution to the magnetization. In this paper, we therefore take it as a reasonable first approximation to calculate quantum spin fluctuations to lowest order in $1/S$ and include the first order corrections to the classical frequencies. We have not addressed the question as to whether other physics, in particular magnon-magnon interaction is introduced to second order in $1/S$.

We compare our results with the inelastic neutron scattering data of Coldea *et al.*⁶ and with the spin wave calculation therein where only nearest neighbor hopping t was considered. We find that including further neighbor hops allows for a more convincing description of the neutron data, with the set of parameters (t, t', t'', U) that best describe the data being comparable to other estimates for cuprate materials. Our analysis also gives a new estimate for the total staggered magnetic moment which is in good quantitative agreement with the experimental estimate⁴⁴.

We now describe in more detail the main features of the data that must be explained and how going beyond the nearest-neighbor hopping provides a better model. The inelastic neutron scattering data of Coldea *et al.*⁶ provide an extensive description of the magnon dispersion in La_2CuO_4 over the whole of the 1st Brillouin zone. The analysis of Ref. [6] clearly shows that the nearest neighbor spin $S = 1/2$ Heisenberg Hamiltonian does not reproduce the magnon dispersion over the whole zone. Most notably, while a spin wave analysis of the Heisenberg model to order $1/S$ gives a flat magnon dispersion over the interval $\mathbf{q}_{\text{BZ}} \in [(\pi, 0), (\pi/2, \pi/2)]$ (along the antiferromagnetic zone boundary), the experimental results show *negative* (downward) dispersion over this region (see Fig. 3). Going beyond $1/S$ for the Heisenberg model does not explain this negative dispersion feature^{45,46}. Rather, introducing interactions between magnons gives rise to a small *positive* (downward) dispersion over this \mathbf{q}_{BZ} interval^{45,46}. Including terms up to $t(t/U)^3$, which generates second and third neighbor and ring exchange interactions, does however provide the characteristic downward dispersion, and this is what allowed Coldea *et al.* to fit the experimental data within a $1/S$ spin wave analysis^{47,48}. Recent analysis of triplon excitations in the copper oxide based ladder material $\text{La}_4\text{Sr}_{10}\text{Cu}_{24}\text{O}_{41}$ also suggest that ring exchange interactions are present and are of a similar amplitude⁴⁹ to those found in Ref. [6] for La_2CuO_4 .

It is important for the rest of the paper to expand

briefly on this negative dispersion and to give an interpretation for it: the spin-only Hamiltonian, $H_s^{(4)}$, obtained from the Hubbard Hamiltonian, H_H , to order t^4/U^3 , contains first, second and third nearest-neighbor exchanges, J_1 , J_2 and J_3 , respectively, as well as a four-spin ring exchange J_c (see Eq.(16)). Within the Holstein-Primakoff spin-wave approximation, all terms in $H_s^{(4)}$, including the ring exchange, contribute to order $1/S$ quadratic magnon creation/annihilation terms to the resulting quadratic magnon Hamiltonian $H_{s,\text{quad}}^{(4)}$. To this order, the spin wave approximation thus eliminates the original multi-spin (ring exchange) nature of the spin Hamiltonian, $H_s^{(4)}$. As a result, $H_{s,\text{quad}}^{(4)}$ could equally well have been derived from a different spin-only Hamiltonian, H_s^{eff} , containing solely *bilinear*, or pairwise, spin exchange terms only. H_s^{eff} would have exchange terms of the form $J_n^{\text{eff}} \mathbf{S}(0) \cdot \mathbf{S}(\mathbf{r}_n)$, which couple a reference spin $\mathbf{S}(0)$ to an n -nearest neighbor spin at \mathbf{r}_n ^{47,48,50}. The relationship between the J_n^{eff} exchange couplings of H_s^{eff} and the set $\{J_1, J_2, J_3, J_c\}$ of $H_s^{(4)}$ is⁶:

$$\left\{ \begin{array}{l} J_1^{\text{eff}} = J_1 - 2J_c S^2 \\ J_2^{\text{eff}} = J_2 - J_c S^2 \\ J_3^{\text{eff}} = J_3 \end{array} \right\}. \quad (1)$$

where $S = 1/2$, $J_1 = (4t^2/U)(1 - 6t^2/U^2)$, $J_2 = J_3 = 4t^4/U^3$ and $J_c = 80t^4/U^3$, and where the convention $J_n^{\text{eff}} > 0$ means antiferromagnetic exchange⁵¹. We note from Eq. 1 that J_c leads to a “renormalization” of J_2 . In particular, for the $t-U$ Hubbard model, $J_2^{\text{eff}} = -16t^4/U^3$ ($S = 1/2$) is negative for all t/U . The negative value of J_2^{eff} favors ferromagnetic correlations across the diagonal of a plaquette and gives a downward dispersion along $\mathbf{q}_{\text{BZ}} \in [(\pi, 0), (\pi/2, \pi/2)]$ ⁶, as required. In the limit $t/U \rightarrow 0$, one recovers the nearest-neighbor Heisenberg $S = 1/2$ Hamiltonian and the dispersion becomes flat along the zone boundary⁵².

Having provided an explanation for the origin of the negative (downward) dispersion along \mathbf{q}_{BZ} , we can now discuss the effect on the spin wave dispersion of including second nearest-neighbor hopping t' . When passing from the Hubbard model, including t' , to a spin only model, the leading order effect of t' is to generate an antiferromagnetic exchange between second-nearest neighbors that modify J_2 in $H_s^{(4)}$:

$$J_2 \rightarrow J_2 + 4(t')^2/U = 4t^4/U^3 + 4(t')^2/U \quad (2)$$

which in turn modifies J_2^{eff} in the $1/S$ spin-wave approximation in Eq. (1):

$$J_2^{\text{eff}} \rightarrow J_2^{\text{eff}} + 4(t')^2/U = 4(t')^2/U - 16t^4/U^3. \quad (3)$$

So, while for $t' = 0$ the dispersion is downward for all t/U , a nonzero t' competes with this trend since the second nearest-neighbor exchange generated to order $4(t')^2/U$, is antiferromagnetic and frustrating. This means that a sizable increase in t/U is required to achieve a good fit to

the data of Ref. [6] when t' is included in the spin-only Hamiltonian to this order. The same observation has been made from a random phase approximation calculations^{53,54} and also from quantum Monte Carlo calculations⁵⁵, both on the half-filled one band Hubbard model. This evolution puts the best fit value for t/U into the intermediate coupling regime and perhaps very close, or maybe even beyond the critical value for a metal insulator transition. If we estimate this critical value from the value of U at which a finite gap in the density of states persists at finite temperature, then Fig. 5 of Ref. [56] suggests that for $t' = t'' = 0$ on the square lattice, the critical value is $t/U \sim 1/6 = 0.166$. In the variational cluster approximation, which overestimates the effect of interactions, the critical value of t/U is larger but studies as a function of $|t'|$ suggest that frustration leads to a decrease of this value⁵⁷. The same trend as a function of frustration (t') occurs on the anisotropic triangular lattice⁵⁸. Hence, with nonzero t' included in the model and presumably at play in the real material, it is ultimately important that successful fits to experiments on parent insulating compounds lead to *smaller* values of t/U than those where $t' = 0$, contrary to what is found in the references cited above where the third nearest neighbor hopping t'' is equal to zero.

As discussed above, the third neighbor hopping term t'' is estimated to be of the same order as t' in a number of cuprate materials and should therefore also be taken into account²⁵. However, the above discussion on the leading effect of t' might leave one wondering whether a perturbative spin-only Hamiltonian, starting from a half-filled one-band Hubbard model can provide a quantitative microscopic description of La_2CuO_4 at all. It is this very question that has motivated us in pursuing the work reported here, and it is why we have derived the spin-only Hamiltonian H_s from a $t-t'-t''-U$ Hubbard model, including all ring exchanges and hopping processes to order $(1/U)^3$. This procedure generates a large number of further neighbor and ring exchange paths, a small number of which make significant contributions. The main corrections come from terms of order $(t')^2/U$ and $(t'')^2/U$ but we also find that ring exchanges of order $t't''t^2/U^3$ are also significant. The latter, in particular, determine the sign of t'/t'' . Of course, the resulting theory has now two more free parameters (i.e. t' and t'') than the original model⁶ to fit the inelastic neutron scattering data and the reader may therefore not be surprised that we achieve a better fit than in Ref. [6]. However, as we show in Section III, the ensemble of parameters giving the best unbiased fit to the data is in good agreement with the values suggested from other sources for various cuprates^{19,20,21,22,26,40}.

The rest of the paper is organized as follows. In Section II we present the method to obtain a consistent spin representation of the original Hubbard model up to third neighbor hops. As an application, in Section III, we investigate the consequences of applying the method to a general $t - t' - t'' - U$ model by fitting the magnon dis-

persion data of Ref. [6] for La_2CuO_4 . Section III also discusses the procedure to calculate the staggered magnetization operator, and shows that our expansion of the $t-t'-t''-U$ model gives a value of the sublattice magnetization in good agreement with experiment⁴⁴. We conclude the paper in Section IV. We have included a number of appendices to assist the reader with a few technical issues. Appendix A gives the various terms that contribute to the effective spin Hamiltonian with arbitrary t , t' and t'' up to order $1/U^3$. In Appendix B we show that the renormalization factor for the magnetization, coming from charge fluctuations³³ is the same in our approach as that found in an extension of the mean-field Hartree-Fock method of Ref. [59]. Appendix C gives the \mathbf{k} dependence of the various terms coming in the $1/S$ spin-wave calculation. Appendix D discusses the spin-wave velocity renormalization factor, $Z_c(\mathbf{k})$. Appendix E comments on the results of various constrained fits to the spin wave energies.

II. EFFECTIVE SPIN HAMILTONIAN FOR THE $t-t'-t''-U$ HUBBARD MODEL

A derivation of the spin-only effective theory starting from the one band $t-U$ Hubbard model has been given by several authors^{17,18,32,33}. In this section we investigate the effects of including new parameters t' and t'' , for direct hops between second and third nearest neighbors, respectively, on the spin-only effective theory. We first recall the key steps in the unitary transformation method for the $t-U$ Hubbard model. We then apply the method to the $t-t'-t''-U$ model and obtain the modified spin-only Hamiltonian generated by all possible virtual electronic paths up to order $1/U^3$, giving terms of order t^4/U^3 , $(t')^4/U^3$, $(t'')^4/U^3$, $t^2(t')^2/U^3$, $t^2(t'')^2/U^3$, t^2t'/U^3 , and $(t't'')^2/U^3$.

A. Derivation of the spin-only effective Hamiltonian

We begin with a brief review of the derivation of the spin-only Hamiltonian of the one band nearest-neighbor Hubbard Hamiltonian, H_{H} :

$$H_{\text{H}} = T + V \quad (4)$$

$$= -t \sum_{i,j;\sigma} c_{i,\sigma}^\dagger c_{j,\sigma} + U \sum_i n_{i,\uparrow} n_{i,\downarrow}. \quad (5)$$

The first term is the kinetic energy term that destroys an electron of spin σ at nearest neighbor site j and creates one on the nearest-neighbor site i . The second term is the on-site Coulomb energy U for two electrons with opposite spin to be on the same site i and where $n_{i,\sigma} = c_{i,\sigma}^\dagger c_{i,\sigma}$ is the occupation number operator at site i .

As introduced by Harris *et al.*³² and developed further by MacDonald *et al.*¹⁸, the transformation relies on the

separation of the kinetic part T into three terms that respectively increase by 1 (T_1), keep constant (T_0) or decrease by one (T_{-1}) the number of doubly occupied sites.

We write :

$$T = -t \sum_{i,j;\sigma} c_{i,\sigma}^\dagger c_{j,\sigma} = T_1 + T_0 + T_{-1} \quad (6)$$

$$T_1 = -t \sum_{i,j;\sigma} n_{i,\bar{\sigma}} c_{i,\sigma}^\dagger c_{j,\sigma} h_{j,\bar{\sigma}} \quad (7)$$

$$T_0 = -t \sum_{i,j;\sigma} h_{i,\bar{\sigma}} c_{i,\sigma}^\dagger c_{j,\sigma} h_{j,\bar{\sigma}} + n_{i,\bar{\sigma}} c_{i,\sigma}^\dagger c_{j,\sigma} n_{j,\bar{\sigma}} \quad (8)$$

$$T_{-1} = -t \sum_{i,j;\sigma} h_{i,\bar{\sigma}} c_{i,\sigma}^\dagger c_{j,\sigma} n_{j,\bar{\sigma}} \quad (9)$$

where $\bar{\sigma}$ stands for up if σ is down and for down if σ is up. This separation comes from multiplying the kinetic term on the right by $n_{i,\bar{\sigma}} + h_{i,\bar{\sigma}} = 1$ and multiplying on the left by $n_{j,\bar{\sigma}} + h_{j,\bar{\sigma}} = 1$.

Applying the unitary transformation $e^{i\mathcal{S}}$ to H_{H} leads to an effective Hamiltonian, \tilde{H}_{S} , where double occupancy is eliminated perturbatively, order by order in \mathcal{S} . Using the relation:

$$\tilde{H}_{\text{S}}^{(k)} = e^{i\mathcal{S}} H_{\text{H}} e^{-i\mathcal{S}} = H_{\text{H}} + \frac{[i\mathcal{S}, H_{\text{H}}]}{1!} + \frac{[i\mathcal{S}, [i\mathcal{S}, H_{\text{H}}]]}{2!} + \dots \quad (10)$$

and, defining as in Ref. [18]

$$T^{(k)}(m_1, m_2, \dots, m_k) = T^k[m] = T_{m_1} T_{m_2} \dots T_{m_k}, \quad (11)$$

\mathcal{S} is solved for, order by order. Hence, starting from a low energy vacuum of singly occupied sites, \tilde{H}_{S} contains no terms that create or annihilate doubly occupied sites up to the order for which \mathcal{S} has been determined. This leads to an expression for \tilde{H}_{S} to order $t(t/U)^3$ (see Refs. [18, 33]):

$$\begin{aligned} \tilde{H}_{\text{S}}^{(4)} = & -\frac{1}{U} T^{(2)}(-1, 1) \\ & + \frac{1}{U^2} T^{(3)}(-1, 0, 1) \\ & + \frac{1}{U^3} \left(T^{(4)}(-1, 1, -1, 1) - T^{(4)}(-1, 0, 0, 1) \right. \\ & \left. - \frac{1}{2} T^{(4)}(-1, -1, 1, 1) \right), \end{aligned} \quad (12)$$

where the associated generator for the unitary transformation is:

$$\begin{aligned} i\mathcal{S}^{(3)} = & \frac{1}{U} (T_1 - T_{-1}) + \frac{1}{U^2} ([T_1, T_0] - [T_0, T_{-1}]) \\ & + \frac{1}{U^3} (-[T_0, [T_0, T_1]] - [T_0, [T_1, T_0]] - [T_1, [T_1, T_0]]) \\ & - \frac{1}{4} [T_{-1}, [T_0, T_{-1}]] + \frac{2}{3} [T_1, [T_1, T_{-1}]] \\ & + \frac{2}{3} [T_{-1}, [T_1, T_{-1}]] \end{aligned} \quad (13)$$

B. Derivation of the spin Hamiltonian.

The effective Hamiltonian $\tilde{H}_s^{(4)}$ in Eq. (12) is still defined in terms of fermion operators entering the $T^{(k)}$ operators. When focusing on the magnetic properties of the half-filled Hubbard model, it is convenient to recast the effective Hamiltonian \tilde{H}_s in Eq. (12) in a spin-only notation. For this, we use a mapping¹⁸ between the subspace of the Hubbard model with singly occupied sites and the Hilbert space of a spin $S = 1/2$ system. The mapping is:

$$\begin{array}{ccc} \text{Hubbard Space} & & \text{Spin } \frac{1}{2} \text{ Space} \\ \\ n_{i,\uparrow} = 1 & \longrightarrow & \left| \cdots \underbrace{\uparrow}_{\text{site } i} \cdots \right\rangle \\ \\ n_{i,\downarrow} = 1 & \longrightarrow & \left| \cdots \underbrace{\downarrow}_{\text{site } i} \cdots \right\rangle \end{array} \quad (14)$$

The spin Hamiltonian $H_s^{(k)}$ acting on this space is derived from the Hamiltonian acting on the occupation number subspace (see Ref. 18 for more details). Once it is written in the spin 1/2 basis it can be transformed into an explicitly SU(2) invariant form using:

$$H_s^{(k)} = \frac{1}{2^N} \sum_{\alpha_1, \alpha_2, \dots, \alpha_N=0}^3 \left(\prod_{l=1}^N \sigma_{\alpha_l}^{(l)} \right) \text{Tr}(\sigma_{\alpha_1}^{(1)} \cdots \sigma_{\alpha_N}^{(N)} \tilde{H}^{(k)}), \quad (15)$$

where $\sigma_{\alpha_p}^{(p)}$ is the Pauli matrix for site p , with electron in spin state α_p . From this one finds the spin-only Hamiltonian evaluated to third order in t/U for the $t-U$ Hubbard model^{18,33}:

$$\begin{aligned} H_s^{(4)} &= \left(\frac{4t^2}{U} - \frac{24t^4}{U^3} \right) \sum_{\langle i,j \rangle} (\mathbf{S}_i \cdot \mathbf{S}_j) \\ &+ \frac{4t^4}{U^3} \sum_{\langle\langle i,j \rangle\rangle} (\mathbf{S}_i \cdot \mathbf{S}_j) \\ &+ \frac{4t^4}{U^3} \sum_{\langle\langle\langle i,j \rangle\rangle\rangle} (\mathbf{S}_i \cdot \mathbf{S}_j) \\ &+ \frac{80t^4}{U^3} \sum_{\langle i,j,k,l \rangle} \left\{ (\vec{S}_i \cdot \vec{S}_j) (\vec{S}_k \cdot \vec{S}_l) \right. \\ &\quad \left. + (\vec{S}_i \cdot \vec{S}_l) (\vec{S}_k \cdot \vec{S}_j) - (\vec{S}_i \cdot \vec{S}_k) (\vec{S}_j \cdot \vec{S}_l) \right\} \end{aligned} \quad (16)$$

where $\langle i, j \rangle$, $\langle\langle i, j \rangle\rangle$, and $\langle\langle\langle i, j \rangle\rangle\rangle$ denote sums over first, second and third nearest neighbors, respectively and where $\langle i, j, k, l \rangle$ identifies a square plaquette with sites i, j, k, l defining the four corners of an elementary square plaquette.

C. Inclusion of t' and t''

Having reviewed the procedure for deriving $H_s^{(k)}$ for nearest-neighbor hopping t only, we now discuss how to include second and third nearest neighbor hopping t' and t'' . We start with an extended Hubbard Hamiltonian:

$$\begin{aligned} H_H &= T + T' + T'' + V \\ &= -t \sum_{i,j_1;\sigma} c_{i,\sigma}^\dagger c_{j_1,\sigma} - t' \sum_{i,j_2;\sigma} c_{i,\sigma}^\dagger c_{j_2,\sigma} \\ &\quad - t'' \sum_{i,j_3;\sigma} c_{i,\sigma}^\dagger c_{j_3,\sigma} + U \sum_i n_{i,\uparrow} n_{i,\downarrow}, \end{aligned} \quad (17)$$

where t' is the hopping constant to the 2^{nd} nearest neighbor and t'' to the 3^{rd} nearest neighbor (see Fig. 1); j_α is the α nearest neighbor of i . As above, we define the operators T_m , taking into account t' and t'' :

$$T_1 = \frac{1}{2} \sum_{i,j;\sigma} (-t_{i,j}) n_{i,\bar{\sigma}} c_{i,\sigma}^\dagger c_{j,\sigma} h_{j,\bar{\sigma}}, \quad (19)$$

$$\begin{aligned} T_0 &= \frac{1}{2} \sum_{i,j;\sigma} (-t_{i,j}) \left(h_{i,\bar{\sigma}} c_{i,\sigma}^\dagger c_{j,\sigma} h_{j,\bar{\sigma}} \right. \\ &\quad \left. + n_{i,\bar{\sigma}} c_{i,\sigma}^\dagger c_{j,\sigma} n_{j,\bar{\sigma}} \right), \end{aligned} \quad (20)$$

$$T_{-1} = \frac{1}{2} \sum_{i,j;\sigma} (-t_{i,j}) h_{i,\bar{\sigma}} c_{i,\sigma}^\dagger c_{j,\sigma} n_{j,\bar{\sigma}}, \quad (21)$$

where $t_{i,j} = t$ if i and j are nearest neighbors, $t_{i,j} = t'$ if i and j are second nearest neighbors, and $t_{i,j} = t''$ if i and j are third nearest neighbors and 0 otherwise. The commutation relations in (10) do not change and the expression for the unitary transformation in (13) remains formally the same. On the other hand, the resulting spin Hamiltonian gets drastically modified by the inclusion of t' or t'' . In particular, many new *plaquette* or ring exchange terms are generated. The complete expression for the spin Hamiltonian is reported in Appendix (A). As in previous work^{18,33}, and even more so here, given the much increased complexity of the Hamiltonian, a computer program was used to collect together all the terms in the projection of Eq. 15 which ultimately lead to a globally SU(2) invariant effective spin-only Hamiltonian $H_s^{(4)}(t, t', t'', U)$.

III. PHYSICAL RESULTS

A. Spin wave dispersion

1. Spin wave calculation

In order to obtain the magnetic excitation spectra presented in Fig. 3 and Fig. 4 we perform a $1/S$ spin wave calculation. The spin operators are written in terms of

boson operators through a Holstein-Primakoff^{60,61} $1/S$ expansion for a bipartite Néel ordered square lattice:

$$\begin{cases} \text{Sublattice a} \\ S_i^z = S - a_i^\dagger a_i \\ S_i^+ = \sqrt{2S - a_i^\dagger a_i} a_i \\ S_i^- = a_i^\dagger \sqrt{2S - a_i^\dagger a_i} \end{cases} \begin{cases} \text{Sublattice b} \\ S_j^z = -S + b_j^\dagger b_j \\ S_j^- = \sqrt{2S - b_j^\dagger b_j} b_j \\ S_j^+ = b_j^\dagger \sqrt{2S - b_j^\dagger b_j} \end{cases} \quad (22)$$

In reciprocal space, one obtains to order S the following general expression of the spin Hamiltonian $H_s^{(4)} \approx H_{s,0}^{(4)} \mathbb{1} + H_{s,\text{quad}}^{(4)}$, where $H_{s,0}^{(4)}$ is the classical ground state energy and $H_{s,\text{quad}}^{(4)}$ is given by

$$H_{s,\text{quad}}^{(4)} = \sum_{\mathbf{k}} A_{\mathbf{k}} \left(a_{\mathbf{k}}^\dagger a_{\mathbf{k}} + b_{\mathbf{k}}^\dagger b_{\mathbf{k}} \right) + B_{\mathbf{k}} \left(a_{\mathbf{k}}^\dagger b_{\mathbf{k}}^\dagger + a_{\mathbf{k}} b_{\mathbf{k}} \right). \quad (23)$$

Note that here and elsewhere in the paper, the sums in reciprocal space are over the magnetic Brillouin zone, which for a square lattice with N spins contains $N/2$ sites. $H_{s,\text{quad}}^{(4)}$ can be diagonalized through a Bogoliubov transformation

$$\begin{cases} a_{\mathbf{k}} = u_{\mathbf{k}} \alpha_{\mathbf{k}} + v_{\mathbf{k}} \beta_{\mathbf{k}}^\dagger \\ b_{\mathbf{k}} = u_{\mathbf{k}} \beta_{\mathbf{k}} + v_{\mathbf{k}} \alpha_{\mathbf{k}}^\dagger \end{cases}, \quad (24)$$

giving

$$H_{s,\text{quad}}^{(4)} = \sum_{\mathbf{k}} \epsilon_{\mathbf{k}} (\alpha_{\mathbf{k}}^\dagger \alpha_{\mathbf{k}} + \beta_{\mathbf{k}}^\dagger \beta_{\mathbf{k}} + 1). \quad (25)$$

and where

$$\begin{aligned} u_{\mathbf{k}}^2 &= \frac{B_{\mathbf{k}}^2}{2\epsilon_{\mathbf{k}}(A_{\mathbf{k}} - \epsilon_{\mathbf{k}})} \\ v_{\mathbf{k}}^2 &= \frac{A_{\mathbf{k}} - \epsilon_{\mathbf{k}}}{2\epsilon_{\mathbf{k}}}. \end{aligned} \quad (26)$$

The magnons for a given wave vector \mathbf{k} are thus two fold degenerate with eigenfrequencies⁶⁰:

$$\epsilon_{\mathbf{k}} = \sqrt{A_{\mathbf{k}}^2 - B_{\mathbf{k}}^2}. \quad (27)$$

In this expression, the functions $A_{\mathbf{k}}$ and $B_{\mathbf{k}}$ take into account all the bilinear and ring exchange interactions entering $H_s^{(4)}$ and given in Appendix A. Detailed expressions for $A_{\mathbf{k}}$ and $B_{\mathbf{k}}$ can be found in Appendix C.

The staggered magnetization operator, M_s^\dagger , is, in reference to sublattice a, defined conventionally for a spin-only Hamiltonian as

$$M_s^\dagger = \frac{1}{(N/2)} \sum_{i=1}^{i=N/2} S_i^z. \quad (28)$$

Rewriting the previous equation in \mathbf{k} space and introducing the Bogoliubov transformation above, we arrive at a

standard expression⁶⁰:

$$\begin{aligned} M_s^\dagger &= S - \frac{2}{N} \sum_{\mathbf{k}} a_{\mathbf{k}}^\dagger a_{\mathbf{k}} = S - \frac{2}{N} \sum_{\mathbf{k}} (u_{\mathbf{k}}^2 \alpha_{\mathbf{k}}^\dagger \alpha_{\mathbf{k}} + v_{\mathbf{k}}^2 \beta_{\mathbf{k}} \beta_{\mathbf{k}}^\dagger \\ &\quad + \text{off-diagonal terms}). \end{aligned} \quad (29)$$

At zero temperature, all $\langle \alpha_{\mathbf{k}}^\dagger \alpha_{\mathbf{k}} \rangle$ and $\langle \beta_{\mathbf{k}}^\dagger \beta_{\mathbf{k}} \rangle$ are zero, and one has for the ground state expectation value of M_s^\dagger , $\langle M_s^\dagger \rangle$:

$$\begin{aligned} \langle M_s^\dagger \rangle &= S - \frac{2}{N} \sum_{\mathbf{k}} v_{\mathbf{k}}^2 \\ &= S + \frac{1}{2} - \frac{2}{N} \sum_{\mathbf{k}} \frac{A_{\mathbf{k}}}{2\epsilon_{\mathbf{k}}}. \end{aligned} \quad (30)$$

2. Magnon self energy: renormalization factor $Z_c(\mathbf{k})$

The $1/S$ correction to Eq. (30) vanishes for the Heisenberg antiferromagnet, with the next corrections appearing at order $1/S^2$ only⁴³. This explains why spin wave calculations give a very good estimate of zero point quantum fluctuations in this model. On the other hand, the terms to quartic order in magnon operators in $H_s^{(4)}$ give a contribution to the diagonal part of the magnon self energy⁴³. This gives rise to a $1/S$ correction to the spin-wave energies $\epsilon_{\mathbf{k}}$ in Eq. (27). This renormalization of the magnon energy scale is important for the quantitative comparison between our calculation and the experimental results of Coldea *et al.*⁶ and for the subsequent determination of the parameters $\{t, t', t'', U\}$ and hence we evaluate it for our effective spin Hamiltonian.

Expanding the spin Hamiltonian to fourth order in the boson operators of the Holstein-Primakoff transformation, one finds:

$$H_s^{(4)} = H_0^{(4)} + H_{s,\text{quad}}^{(4)} + H_{s,\text{quart}}^{(4)}. \quad (31)$$

$H_{s,\text{quart}}^{(4)}$ is now treated as a first order perturbation to the quadratic spin-wave Hamiltonian $H_{s,\text{quad}}^{(4)}$. To this order the magnon energy is shifted but the eigenvectors are unchanged and magnon-magnon interactions are not generated. The shift is found by diagonalizing the set of 2×2 matrices with elements $\langle 0 | \gamma_{\mathbf{k}} H_{s,\text{quart}}^{(4)} \gamma_{\mathbf{k}}^\dagger | 0 \rangle$, where $(\gamma_{\mathbf{k}}, \gamma_{\mathbf{k}}') \in \{\alpha_{\mathbf{k}}, \beta_{\mathbf{k}}\}$. We hence find a correction $\delta\epsilon_{\mathbf{k}}$ to the magnon energy, and a renormalized magnon energy $\tilde{\epsilon}(\mathbf{k})$:

$$\epsilon_{\mathbf{k}} \longrightarrow \tilde{\epsilon}_{\mathbf{k}} = \epsilon_{\mathbf{k}} + \delta\epsilon_{\mathbf{k}} = \epsilon_{\mathbf{k}}(1 + \Delta_{\mathbf{k}}) = \epsilon_{\mathbf{k}} Z_c(\mathbf{k}), \quad (32)$$

where we refer to $\Delta_{\mathbf{k}}$ as the magnon energy correction and $Z_c(\mathbf{k})$ the magnon energy renormalization factor. For the Heisenberg model, the product $\epsilon_{\mathbf{k}} \Delta_{\mathbf{k}}$ corresponds to the leading contribution to the magnon self energy calculated in Ref. [43]. To order t^2/U and with t' and t'' set to zero, $\Delta_{\mathbf{k}}$ is uniform over the whole Brillouin Zone and we find:

$$Z_c(\mathbf{k}) \simeq 1.1579, \quad (33)$$

as obtained in Ref. [43]. Details of this calculation are given in Appendix D.

When non-zero values of t' and t'' are included, $\Delta_{\mathbf{k}}$ is no longer constant over the Brillouin zone, but the two-fold degeneracy for each wave vector \mathbf{k} remains. The renormalizing factors $Z_c(\mathbf{k})$ are calculated numerically. For a given set of t' and t'' values, a finite size scaling analysis was used to extrapolate the sums over \mathbf{k}' in Appendix D over the Brillouin zone to the thermodynamic limit. In Fig. 2 we show the dispersion of $Z_c(\mathbf{k})$ obtained for the parameter set (t, t', t'', U) (see Eq. 38) giving the best fit to the magnon dispersion data⁶ from Coldea *et al.*, as described in the next section. For these values the mean value of $\Delta_{\mathbf{k}}$ over the Brillouin zone is found to be

$$\langle Z_c(\mathbf{k}) \rangle \simeq 1.219. \quad (34)$$

We also calculate the dispersion of $\Delta_{\mathbf{k}}$ over the Brillouin zone for this set of parameters, finding:

$$\frac{\sigma(\Delta_{\mathbf{k}})}{\langle \Delta_{\mathbf{k}} \rangle_{\mathbf{k}}} \simeq 0.33 \times 10^{-3}. \quad (35)$$

where σ is the standard deviation of the distribution of values. Details of the calculation can be found in Appendix D.

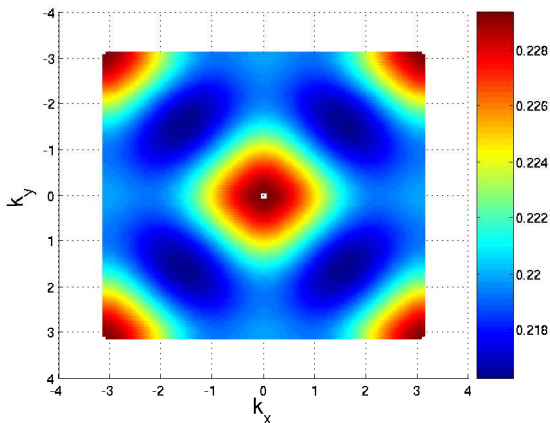


FIG. 2: (Color online) \mathbf{k} dependence of $\Delta_{\mathbf{k}}$. Data is shown over the structural Brillouin zone of the square lattice. As can be seen, the dispersion has the symmetry of the zone corresponding to the antiferromagnetic order.

From our results here one can see that the magnon energy renormalization $Z_c(\mathbf{k})$, calculated to order $1/S$, is indeed an important element of the quantitative comparison between our microscopic theory and the experimental results of Coldea *et al.*⁶. The values obtained for $Z_c(\mathbf{k})$ change the energy scale of the magnon dispersion by around 20% of what would have been obtained if the bare $Z_c(\mathbf{k}) = 1$ had been used. The Z_c factors therefore have proportionate consequences for the values of U and t deduced by comparisons with experiment.

3. Experimental data and previous results

The magnon energy spectrum for La_2CuO_4 obtained through inelastic neutron scattering⁶ is shown in Fig. 3. The data follow a trajectory through the Brillouin zone covering, in particular, the line along the magnetic zone boundary with wave vector in the interval $\mathbf{q}_{\text{BZ}} = [(\pi, 0), (\pi/2, \pi/2)]$, where the previously discussed downward dispersion is manifest. Also included in this figure is the fit of Ref. [6] using the Hamiltonian (16). The parameters used there to make the fit at a temperature of 10 K are⁶

$$\left\{ \begin{array}{l} t/U = 0.135 \pm 0.03 \\ t = 0.30 \pm 0.02 \text{ eV} \\ U = 2.3 \pm 0.4 \text{ eV} \end{array} \right\}. \quad (36)$$

While the above fit of Coldea *et al.*⁶ is clearly good, the numerical values should be compared with those from experiments and band calculations on other cuprate materials. For example, values found by fitting ARPES results for the half-filled compound $\text{Sr}_2\text{CuO}_2\text{Cl}_2$ containing CuO_2 planes are^{22,39,40}

$$\left\{ \begin{array}{l} t/U = 0.1 \pm 0.05, \\ t'/t = -0.35 \pm 0.05, \\ t''/t = 0.22 \pm 0.05, \\ t = 0.35 \text{ eV} \\ U = 3.5 \text{ eV} \end{array} \right\}. \quad (37)$$

One can see that the energy scale, set by U and the ratio t/U in Eq. (37) are quite different from that found by Coldea *et al.*⁶. Also, while the effects of t' and t'' are neglected in Ref. [6], the ARPES results unambiguously show that t' and t'' have non-negligible values within the CuO_2 planes^{22,40}, although band structure calculations^{24,25,41} on LaCu_2O_4 and ARPES experiments on the lightly doped system^{19,20,21,22} do suggest somewhat smaller values of t' than those in Eq. (37) for $\text{Sr}_2\text{CuO}_2\text{Cl}_2$. In other words, based on various experiments on a number of cuprates, one would have “anticipated” a t/U value for La_2CuO_4 somewhat smaller than the value in Eq. (36) from Ref. [6], although the experimental uncertainty allows for some overlap between the two. Most importantly, from a theoretical point of view, $t/U = 0.135$ corresponds to $U = 7.4t$, which is smaller than the tight binding band width of $8t$. This value may therefore be a little small⁵⁶, to insure that the material remains within the Mott insulating phase. The error bars do allow values up to $U = 9.5$ ($t/U = 0.105$), which would push the model further into the insulating regime. Nevertheless, it is quite possible that the analysis of the data in Ref. (6) using the model $H_s^{(4)}$ in Eq. (16) leads to an underestimation of U .

From this discussion it is clear that a more detailed analysis of the experimental magnon dispersion that accounts for t' and t'' is needed.

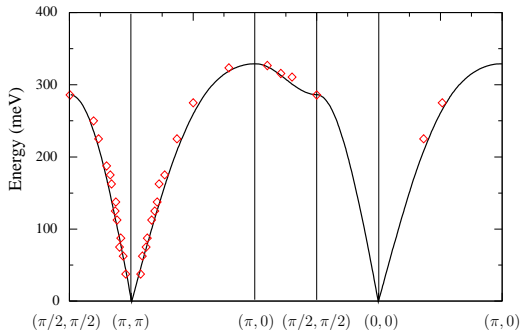


FIG. 3: (Color online) Magnon energy in La_2CuO_4 , as a function of wave vector \mathbf{k} , across the Brillouin zone at a temperature of 10 K. The experimental data (red squares) and fit (full line) are from reference⁶. The $\{t, t', t'', U\}$ fitting parameters are given in (36).

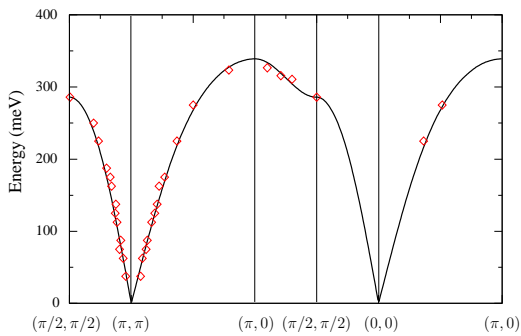


FIG. 4: (Color online) Magnon energy in La_2CuO_4 , as a function of wave vector \mathbf{k} , across the Brillouin zone at a temperature of 10 K. The experimental data (red squares) are from reference⁶. The fit is made using the parameters given by (38).

4. Fitting procedure and fit to the experimental data

Our theory, $H_s^{(4)}(t, t', t'', U)$ in Appendix A, now contains four independent parameters, t, t', t'', U which we fit to the ensemble of experimental data points from Ref. [6]. As we show in Appendix D, $Z_c(\mathbf{k})$ is a function of $t/U, t'/t, t''/t$ and \mathbf{k} . It thus should be calculated over the ensemble of data points for each iteration of the fitting algorithm. As the expression for $Z_c(\mathbf{k})$ contains inner sums ($\sum_{\mathbf{k}'}$) over the Brillouin zone, the fitting procedure is time consuming. A finite size scaling analysis of the convergence of these sums towards the thermodynamic limit is discussed in Appendix D. The fitting procedure is as follows. We choose a first point at wave vector \mathbf{k} with experimental magnon energy $\epsilon_{\text{exp}}(\mathbf{k})$ and minimize the quantity $\delta(\mathbf{k}) = |\tilde{\epsilon}(\mathbf{k}) - \epsilon_{\text{exp}}(\mathbf{k})|$ with respect to t, t', t'', U . From this first fit we extract a factor $4t^2/U$ that fixes the energy scale for the ensemble of points and allows us to write $\tilde{\epsilon}(\mathbf{k})$ as $(4t^2/U)$ times a function of $t/U, t'/t, t''/t$ and \mathbf{k} . This energy scaling step can be achieved for many values of $t/U, t'/t$ and t''/t and the constraints on these variables are not very high at

this stage. The best fit parameter set is now found by minimizing the ensemble of variables $\{\delta(\mathbf{k})(U/4t^2)\}$ with respect to $t/U, t'/U, t''/U$, using least squares fit. Once the final value of t/U is established, the value of t , and hence U, t' and t'' , are deduced. The values found are:

$$\left\{ \begin{array}{l} t/U = 0.126 \pm 0.03, \\ t'/t = -0.327 \pm 0.05, \\ t''/t = 0.153 \pm 0.05, \\ t = 0.422 \text{ eV} \\ U = 3.34 \text{ eV} \end{array} \right\}. \quad (38)$$

The error bars, obtained through the calculation of the least-squares function χ^2 , represent a deviation of less than 5% from the best fit values.

If the dispersion in $Z_c(\mathbf{k})$ is ignored, it only needs to be calculated once for each iteration of the ensemble of points, thus considerably speeding up the procedure. Ignoring the dispersion and taking $Z_c(\mathbf{k}) = \langle Z_c(\mathbf{k}) \rangle = \text{constant}$, the best fit parameter set for this case gives the values:

$$\left\{ \begin{array}{l} t/U = 0.121 \pm 0.03, \\ t'/t = -0.313 \pm 0.05, \\ t''/t = 0.167 \pm 0.05, \\ t = 0.430 \text{ eV} \\ U = 3.75 \text{ eV} \end{array} \right\}. \quad (39)$$

Comparing the two sets, taking the size of the error bars into account and considering the fact that $Z_c(\mathbf{k})$ represents only the leading correction to the magnon energies, we conclude that the dispersion of $\Delta_{\mathbf{k}}$ does not have a significant effect on the determination of the parameters.

The best fit to the experimental data using parameter set (38) is shown in Fig. (4). Comparing with Fig. (3), one observes that introducing t' and t'' leads to a clear improvement in the quality of the fit through the experimental points. One might have expected this, given the increased number of free parameters. However, comparing the set (38) with (37), one can also see that the parameters correspond more realistically with those thought to describe other cuprates such as, for example, $\text{SrCuO}_2\text{Cl}_2$. This is particularly the case for the energy scales t and U which are found to be larger than those in Eq. (36). The ratios t'/t and t''/t are also in fair agreement with values for other cuprates and, perhaps most interesting, the fitting procedure even finds the correct signs for these ratios. The ratio t/U is slightly reduced compared with (36) and more in line with a value that one would expect for a system in the Mott insulating regime, although the change is less spectacular than in the case of the absolute energy scales t and U , with the difference in the t/U value remaining within the experimental error bars. However, considering the overall comparison between calculations and the experiments of Ref. [6], it would appear that adding all terms in t, t' and t'' up to order $1/U^3$ does allow a quantitative description of the

magnon dispersion in La_2CuO_4 , which is an improvement over the equivalent procedure which only includes the t and U parameters.

5. Comments on the influence of t' and t''

Referring to Appendix A, one can see that the inclusion of t' and t'' and all four hop processes involving t, t' and t'' introduces a large number of new ring exchange terms. From this observation one might ask which of the many terms make the most difference and could we have got away with a less complex effective spin Hamiltonian? In this section we address these questions and justify our choice to do a complete calculation of all four hop processes.

The first question is whether or not we can limit ourselves to just one extra parameter t' or t'' . This point has already been discussed in the Introduction (Section IB). We argued there, (Eq. (3)), that t' increases the strength of the antiferromagnetic second neighbour exchange, $J_2 \rightarrow t^4/U^3 + 4(t')^2/U$. This in turn modifies the effective second neighbour coupling in the spin wave analysis, $J_2^{\text{eff}} \rightarrow 4(t')^2/U - 16t^4/U^3$ making it less strongly ferromagnetic, or even antiferromagnetic if t' is sufficiently large. As the negative magnon dispersion along the zone boundary⁶ is a consequence of a ferromagnetic (i.e. negative) J_2^{eff} , one expects that fitting the calculated magnon dispersion to the experimental data will require a larger value of t/U if $t' \neq 0$ but t'' is ignored. This is indeed the case; introducing t' to order $(t')^2/U$ and setting $t'' = 0$, as well as neglecting all terms of order $(t't)^2/U^3$ and $(t')^4/U^3$, the following best fit parameters are found:

$$\left\{ \begin{array}{l} t/U = 0.166 \pm 0.016, \\ t'/t = -0.24 \pm 0.01, \end{array} \right\}. \quad (40)$$

The results are very close to those found from a random phase approximation^{53,54} and also from quantum Monte Carlo calculations⁵⁵. It is clear that the addition of t' only has taken the parameter set in the wrong direction: t/U is now further from most estimates than the case when $t' = 0$. Also, with $U = 6t$ the system could be very near the metallic phase⁵⁶, and not deep in the Mott insulating phase, as is the case for La_2CuO_4 . As we discussed in the introduction, for $U = 6t$ the $t' = 0$ model is right at the metal-insulator transition and the presence of a finite t' increases even further the value of U necessary to position the system in the insulating phase^{29,57}.

The leading effect of third-neighbor hopping t'' is also to increase an exchange interaction, this time J_3 , through the relation :

$$J_3 = 4\frac{t^4}{U^3} \longrightarrow J_3 = 4\frac{t^4}{U^3} + 4\frac{(t'')^2}{U}. \quad (41)$$

However, in this case antiferromagnetic (positive) exchange also contributes, as does the ring exchange term,

to a negative (downward) dispersion along the magnetic zone boundary. Including just t'' , one would therefore expect the best fit parameters for the data to include a particularly small ratio of t/U , which is indeed the case. Hence we see that, as far as this characteristic dispersion is concerned, t' and t'' play opposing roles. It is therefore clear that one needs to include both hopping constants to get a good fit to the experimental data as we have illustrated in Fig. 4 with parameters (Eq. (37)) similar to those in other cuprates^{23,27,41}.

Given that individually, terms of order t^2t''/U^3 are only one tenth of the magnitude of terms of order t^2/U or of the terms of order t^4/U^3 , one might expect the good fit reported in Section(38) to be also obtained when taking into account terms of order $(t')^2/U$ and $(t'')^2/U$ only, and ignoring the host of more complex four hop terms generated by the further neighbor hopping. Not so! If one neglects them and only considers t' and t'' to order $4(t')^2/U$ and $4(t'')^2/U$, one obtains the following set of best fit parameters:

$$\left\{ \begin{array}{l} t/U = 0.14 \pm 0.03, \\ t'/t = 0 \pm 0.0, \\ t''/t = 0 \pm 0.0, \\ t = 0.303 \text{ eV}, \\ U = 2.14 \text{ eV} \end{array} \right\}. \quad (42)$$

Within numerical error this is the same data set as Coldea *et al.*(36), with $t'/t = t''/t = 0$. The rather surprising and interesting conclusion is therefore that, on their own, the two-hop further neighbor terms make no net contribution. Rather, it is the four-hop processes that make the difference. It seems that their small value is compensated for by their multiplicity; that is, by the fact that a given site i appears in a large number of diagrams of order $1/U^3$. Hence, their contribution is increased by an order of magnitude and in this intermediate coupling regime, the global effect of the near-neighbor four hop terms, the majority of which are ring exchanges, is as important as that for the two hop further neighbor processes (Note that as t' and t'' are both zero in Eq.(42), $Z_c(\mathbf{k})$ is once again given by (33) over the whole zone). An alternative procedure would be to impose some partial constraints on the parameters (t, t', t'', U) , using values obtained from, say, band structure calculations. Results of such fits are briefly discussed in Appendix E.

Finally, we remark that in our fitting procedure, the symmetry is broken between data sets with positive and negative values for the ratio t'/t'' . The best fit occurs for a negative ratio t'/t'' (see Eq. (37)). Recall that a canonical particle-hole transformation at fixed chemical potential changes the sign of all hopping integrals and leaves the filling invariant, since $2 - n = n$ when $n = 1$ ^{3,62}. An additional change of phase of the creation-annihilation operators on one of the sublattices by π restores the sign of nearest-neighbor hopping t , but not that of t' and t'' . This shows that t'/t and t''/t can have arbitrary sign but that the sign of t'/t'' is physically relevant. The symme-

try breaking between positive and negative signs for t'/t'' can only be accessed by including four hop processes. As one can see from Appendix A, most of the spin interaction terms are even in powers of t , t' and t'' . However, a small number of terms have odd powers of t' and t'' . These are the terms that determine the sign of the hopping ratios. This can be seen in Fig. 5 where we show the χ^2 parameter from the fitting algorithm as a function of t'/t and t''/t (the value of t/U being set to the best fit value). If the terms proportional to $t^2 t' t'' / U^3$ are deleted from $H_s^{(4)}$ (see Fig. 5(a)), the χ^2 parameter has four fold symmetry and there are four points of best fit independently of the sign of t'/t and t''/t . On the other hand, when these terms are included (see Fig. 5(b)), the symmetry is clearly broken. The minima for positive ratio t'/t'' become broader and shallower, while those for negative sign are narrower and deeper. The fitting procedure hence favors the two points with a negative sign for the ratio t'/t'' . To lift the remaining degeneracy we have to appeal to band structure calculations^{24,25,41} or ARPES experiments^{19,20,21,22,40}, both of which find t'/t negative, hence t''/t positive.

B. Magnetization and spin Hamiltonian

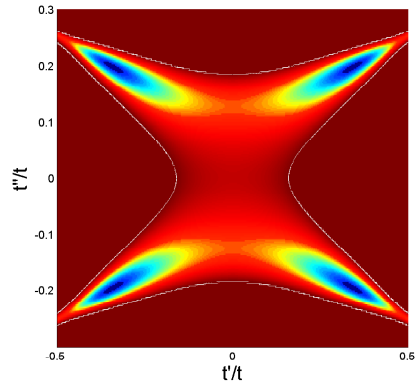
Having found a set of parameters (t, t', t'', U) that suitably describes the experimental spin-wave dispersion data, we now explore how this new set and the derivation of the effective spin Hamiltonian, $H_s^{(4)}(t, t', t'', U)$ affects the value of the zero temperature Néel order parameter.

1. Magnetization operator

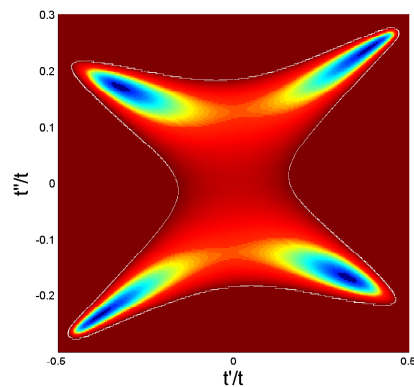
In the construction of effective theories all operators, O_H , defined in the original model must be canonically transformed before they can be exploited in a calculation within the spin only theory. That is, within the effective theory, O_H becomes $O_s = e^{iS} O_H e^{-iS}$ and the expectation value in the ground state is defined by

$$\langle O \rangle = \frac{{}_H \langle 0 | O_H | 0 \rangle_H}{{}_H \langle 0 | 0 \rangle_H} = \frac{{}_s \langle 0 | O_s | 0 \rangle_s}{{}_s \langle 0 | 0 \rangle_s}. \quad (43)$$

Here $|0\rangle_H$ and $|0\rangle_s = e^{iS}|0\rangle_H$ are the ground state wave vectors in the original Hubbard (H) and spin-only (S) models. We have recently shown³³ that incorporating this transformation has important consequences for the ground state magnetization as one moves into the intermediate coupling regime. On application of this procedure on the magnetization operator we find³³ new quantum fluctuations arising from the charge delocalization over closed virtual loops of electronic hops. These spin independent fluctuations allow us to reconcile an apparent paradox concerning the behavior of the ground state magnetization, as a function of t/U . As discussed above, the leading effect of including processes to order $t(t/U)^3$



(a) χ^2 with odd powers of t'/t and t''/t excluded



(b) χ^2 with odd powers of t'/t and t''/t included

FIG. 5: (Color online) Goodness of fit parameter χ^2 (grey scale) as a function t''/t and t'/t with the terms with odd powers of t'/t and t''/t excluded (5(a)) and included (5(b))

is to introduce effective second and third neighbor spin interactions (see Eq. (1)). Within the lowest $1/S$ order spin wave approximation, the resulting effective ferromagnetic second neighbor interaction reduces the transverse quantum spin fluctuations and stabilizes the Néel order of the spin model. This would naively seem to imply that the staggered magnetization should be an increasing function of t/U as the system departs from the Heisenberg limit, $t/U \rightarrow 0$; a result which is difficult to justify on physical grounds. Indeed, one might expect that as t/U is increased, the enhanced electron mobility would lead to a progressive return to the non-magnetic metallic state, with the staggered moment decreasing as t/U increases, as found in Ref. [59], rather than increasing. In Ref. [33] we showed that this is indeed the case: the new quantum fluctuations, or “charge fluctuation” channel, arising from virtual doubly occupied

states, counter the effect of generating a ferromagnetic second neighbor interaction. Consequently, the ground state magnetization for the Hubbard model, when calculated using the spin-only description, is indeed a decreasing function of t/U . The main steps of the calculation are reviewed below and then extended to include the hopping parameters t' and t'' .

Within the Hubbard Hilbert space, the staggered magnetization operator M_H^\dagger is defined by:

$$M_H^\dagger = \frac{1}{N} \sum_i S_i^z e^{-i\mathbf{Q}\cdot\mathbf{r}_i}, \quad (44)$$

where:

$$\mathbf{Q} = (\pi, \pi) \text{ and } S_i^z = \frac{1}{2} \sum_{s_1, s_2} c_{i, s_1}^\dagger \sigma_{s_1, s_2}^z c_{i, s_2}. \quad (45)$$

The magnetization in the ground state $|0\rangle_H$ of the Hubbard model is defined as:

$$M = {}_H\langle 0 | M_H^\dagger | 0 \rangle_H. \quad (46)$$

Working within the effective spin theory, we have to express all the operators in the spin language. Mathematically this means that the unitary transformation in (13) has to be applied to all operators including M_H^\dagger :

$$M_s^\dagger = e^{iS} M_H^\dagger e^{-iS}. \quad (47)$$

The commutation relations between M_H^\dagger and the different operators in (13) are⁷⁷

$$[T_1, M_H^\dagger] \doteq \frac{1}{N} \tilde{T}_1 = \frac{t}{N} \sum_{i, j, \sigma} n_{i, \bar{\sigma}} c_{i, \sigma}^\dagger c_{j, \sigma} h_{i, \bar{\sigma}} (-1)^i \hat{\sigma}_{\sigma, \sigma}^z, \quad (48)$$

$$[T_{-1}, M_H^\dagger] \doteq \frac{1}{N} \tilde{T}_{-1} = \frac{t}{N} \sum_{i, j, \sigma} h_{i, \bar{\sigma}} c_{i, \sigma}^\dagger c_{j, \sigma} n_{i, \bar{\sigma}} (-1)^i \hat{\sigma}_{\sigma, \sigma}^z, \quad (49)$$

$$[T_0, M_H^\dagger] \doteq \frac{1}{N} \tilde{T}_0 = \frac{t}{N} \sum_{i, j, \sigma} \left(n_{i, \bar{\sigma}} c_{i, \sigma}^\dagger c_{j, \sigma} n_{i, \bar{\sigma}} (-1)^i \hat{\sigma}_{\sigma, \sigma}^z + h_{i, \bar{\sigma}} c_{i, \sigma}^\dagger c_{j, \sigma} h_{i, \bar{\sigma}} (-1)^i \hat{\sigma}_{\sigma, \sigma}^z \right). \quad (50)$$

Expressed in terms of these operators, the staggered magnetization operator reads³³:

$$M_s^\dagger = M + \frac{1}{U} \left(\tilde{T}_1 - \tilde{T}_{-1} \right) + \frac{1}{2U^2} \left(\tilde{T}_{-1} T_1 - T_{-1} \tilde{T}_1 \right). \quad (51)$$

The symmetry associated with half filling ensures that contributions to this expression corresponding to odd numbers of hops, such as the second term in the right-hand side of Eq. (51), are zero. Writing the expression

in terms of $S = 1/2$ spin operators³³ we find:

$$M_s^\dagger = \frac{1}{N} \left(\sum_i S_i^z e^{i\mathbf{Q}\cdot\mathbf{r}_i} - \frac{2t^2}{U^2} \sum_{\langle i, j \rangle} \{ S_i^z - S_j^z \} e^{i\mathbf{Q}\cdot\mathbf{r}_i} \right). \quad (52)$$

In the case of periodic boundaries, or in the thermodynamic limit where boundaries can be neglected, all sites become equivalent and the correction to the magnetization operator becomes a multiplicative factor³³:

$$M_s^\dagger = \tilde{M}_s^\dagger \left(1 - 8 \frac{t^2}{U^2} \right), \quad (53)$$

where $\tilde{M}_s^\dagger = \frac{1}{N} \sum_i S_i^z e^{i\mathbf{Q}\cdot\mathbf{r}_i}$ is the naive expression for the magnetization operator in the spin language³³.

2. Role of t' and t''

Inclusion of the higher order hopping constants t' and t'' introduces extra paths for charge delocalization and we might expect new charge fluctuation terms to appear. The hopping operators T_m in Eqs. (19,20,21), can be generalized to include t' and t'' and the commutation relations in Eqs. (48,49,50) are redefined:

$$[T_m, M_H^\dagger] \doteq \frac{1}{N} \tilde{T}_m, \quad (54)$$

$$[T'_m, M_H^\dagger] \doteq \frac{1}{N} \tilde{T}'_m, \quad (55)$$

$$[T''_m, M_H^\dagger] \doteq \frac{1}{N} \tilde{T}''_m, \quad (56)$$

for hops involving t, t' and t'' , respectively. The staggered magnetization operator (51) is thus also generalized. Dropping the first order terms in $1/U$ that do not contribute to the expectation value in a singly-occupied state, M_s^\dagger takes the form:

$$M_s^\dagger = M + \frac{1}{2U^2} \left\{ \left(\tilde{T}_{-1} + \tilde{T}'_{-1} + \tilde{T}''_{-1} \right) (T_1 + T'_1 + T''_1) - (T_{-1} + T'_{-1} + T''_{-1}) \left(\tilde{T}_1 + \tilde{T}'_1 + \tilde{T}''_1 \right) \right\}. \quad (57)$$

However, it turns out that the operators \tilde{T}'_m and \tilde{T}''_m defined in Eqs. (55,56) are identically equal to $\hat{\mathbf{0}}$ ⁷⁸. From this result, it follows that the first corrections to Eq. (53) that depend on t' and t'' appear beyond the second order in the perturbation scheme. Hence we find that to order $(t''/U)^2$ the expression for $M_s^\dagger(t, t', t'')$ is unchanged and given by Eq. (53). However, this does not mean that introducing t' and t'' has no effect on the expectation

value for the staggered magnetization. Firstly, the inclusion of t' and t'' in the magnon dispersion modifies the ensemble of parameters (t, t', t'', U) that best fit the data. Secondly, the zero point fluctuations are controlled by $(t/U, t'/t, t''/t)$, through the \mathbf{k} dependence of $u_{\mathbf{k}}, v_{\mathbf{k}}, A_{\mathbf{k}}$ and $B_{\mathbf{k}}$ in Section III A 1 and this, as we discuss below, directly affects M_s^\dagger .

The charge renormalization factor has also been calculated using a Hartree-Fock mean-field method as in Ref. [59], in which transverse spin fluctuations are neglected (see Appendix B). This calculation on a square lattice gives the same factor, $1 - 8(t/U)^2$, independently of t' and t'' . Physically this comes about because, in the spin-density wave ground state (i.e. Néel order, $\mathbf{Q} = (\pi, \pi)$), electron hops between two sites that belong to the same Néel ordered sublattice are prohibited by the Pauli principle. Hence, same-sublattice hops by t' and t'' do not contribute to charge renormalization to order $(t')^2/U, (t'')^2/U$.

3. Consequences

An experimental estimate of the zero temperature sublattice ordered moment in La_2CuO_4 has been determined from neutron scattering. Lee *et al.*⁴⁴ find

$$M_{\text{experiment}} = g \langle M_s^\dagger \rangle \mu_B = 0.55 \pm 0.05 \mu_B, \quad (58)$$

where g is the Cu^{2+} Landé g -factor. The g -factor for Cu^{2+} in layered cuprates such as La_2CuO_4 has apparently not been determined experimentally⁶³. However, a typical value for a distorted octahedral environment is given by Abragam and Bleaney⁶⁴, $g \simeq 2.2$. We use this value to compare theoretical estimates of the ordered moment with the experimental value. A spin wave calculation for the nearest-neighbor Heisenberg antiferromagnet gives^{2,65,66} $\langle M_s^\dagger \rangle^{\text{nn}} \simeq 0.304$, which is in good agreement with the value obtained from quantum Monte Carlo. This gives for the moment, $M^{\text{sw}} = g \langle M_{\text{sw}}^\dagger \rangle^{\text{nn}}$, $M^{\text{sw}} \approx 0.67 \mu_B$, well in excess of the above $0.55 \mu_B$ value determined experimentally⁴⁴. Using the parameter set of Coldea *et al.*⁶ but neglecting charge renormalization leads to an *increased* expectation value: $\langle M_s^\dagger \rangle \simeq 0.32$, taking the moment to $0.70 \mu_B$, hence further from the experimental estimate of Ref. [44]. Including the charge renormalization factor³³ $1 - 8t^2/U^2$ of Eq. (53) gives $\langle M_s^\dagger \rangle \simeq 0.27$ and $M^{(t)} \simeq 0.59 \mu_B$ in better agreement with experiment. Including both the charge renormalization and the effects of t' and t'' we find

$$\langle M_s^\dagger \rangle^{(tt't'')} \simeq 0.235, \quad (59)$$

from which we obtain

$$\langle M^\dagger \rangle^{(tt't'')} = g \langle M_s^\dagger \rangle^{(tt't'')} \simeq 0.52 \mu_B, \quad (60)$$

which is in even better agreement with experiment. Given the uncertainty in the experimental measurement

value in Eq. (37) and in the theoretical value that should be taken for g , it is difficult to make in-depth comment on the difference between $\langle M \rangle^{tt't''}$ and $\langle M \rangle^t$. However, the results do serve to illustrate the importance of the charge renormalization at this level of approximation. Here, it is an essential element in the quantitative agreement with experiment, and it is only through the inclusion of spin independent quantum corrections (e.g. virtual double site-occupancy) that quantitative agreement can be achieved.

IV. DISCUSSION

It is known from ARPES measurements and band structure calculations that t' and t'' are not negligible compared to t in a number of copper oxide materials. We have thus introduced second and third neighbor hopping parameters, t' and t'' , into the Hubbard Hamiltonian and included all closed four hop virtual electronic pathways into the canonical transformation to derive an effective spin-only Hamiltonian for the case of a half filled band. This Hamiltonian contains many ring exchange terms. These kinds of terms have been the subject of much discussion lately^{33,34,35,36,37,38}. Through this calculation we are able to test the capacity of the one band Hubbard model to describe the magnetic properties of the antiferromagnetic parent high-temperature superconductor La_2CuO_4 . We find in general good quantitative agreement between the predictions of the $t - t' - t'' - U$ model and experimental measurements of the magnetic properties of the compound⁶⁷.

An exact solution of the spin-only Hamiltonian we have derived is clearly far out of reach. In fact, because of the frustration and ensuing sign problem introduced by the various frustrating bilinear spin-spin couplings and the many ring exchange terms, even a quantum Monte Carlo attack on the low temperature properties of this model seems difficult to envisage in the near future. However, it has long been known that a spin-wave analysis up to leading order in a $1/S$ expansion accurately reproduces the zero temperature staggered moment in the Heisenberg model on a square lattice². This is because of the cancellation of the magnon-magnon interaction terms to second order in $1/S$ for this particular lattice⁴³. This suggested that a similar spin wave analysis can be a good starting point to describe the observed magnetic excitation spectrum in La_2CuO_4 and this is indeed what we have found in this paper.

In our spin wave calculations, we calculated the magnetization to leading order in $1/S$ and included the first order correction to the classical spin wave frequencies. The magnon energies are thus renormalized by a spin-wave renormalization factor $Z_c(\mathbf{k})$. Since the classical spin-wave frequencies are already of order $1/U^3$, we only retained terms of order $t^2/U, (t')^2/U$ and $(t'')^2/U$ in calculating $Z_c(\mathbf{k})$. Hence, to this order, it does not depend on the ring exchange terms which are of order $1/U^3$. In

the end, $Z_c(\mathbf{k})$ raises the energy scale by about 20% over the whole of the Brillouin zone, allowing good agreement between experiment and theory without the introduction of any arbitrary scale factors.

To make contact with experiments on La_2CuO_4 the spin wave calculation was set up starting from the classical antiferromagnetic Néel ground state. Within this framework, the general effect of the ring exchange is to reduce the transverse quantum spin fluctuations rather than increase them (see however the discussion of charge renormalization in the following paragraph). With the parameters coming out of the calculation, we therefore seem far from entering an exotic quantum phase driven from large quantum spin fluctuations about the Néel ordered state. Yet, the ring exchanges are found to play a very important role. In particular, it seems that the large numbers of such terms and their large dimensionless prefactors (see Appendix A) outweighs their small $O(1/U^3)$ amplitude, although a more extensive study is required here to understand this point in detail. Further, ring exchange plays a crucial role in determining the relative sign of the ratios t'/t and t''/t . There is experimental evidence from ARPES measurements and band structure calculations that t'/t is negative while t''/t is positive in a number of cuprates. In our calculation there are terms of order t^2t''/U^3 which break the $t''/t' \rightarrow -t''/t'$ symmetry in the effective spin-only Hamiltonian $H_s^{(4)}$, allowing us to deduce the correct sign for the ratio of t'/t'' compared with experiment. In our procedure, we determined unconstrained values of U, t, t' and t'' by comparing our magnon dispersion data with that from experiments on La_2CuO_4 ⁶. The best fit is found with one positive (t''/t) and one negative (t'/t') ratio, exactly as in ARPES experiments and band calculations and, for example, our best fit data set is in good agreement with those from the ARPES experiments on $\text{Sr}_2\text{CuO}_2\text{Cl}_2$ (compare Eq.(38) with Eq.(37)).

At the level of approximation at which the canonical transformation is performed^{18,32,33}, finite charge mobility renormalizes the magnetic moment calculated from the spin only Hamiltonian by a factor $(1 - 8t^2/U)$ ³³. We found that t' and t'' do not contribute further to this factor. This is because direct second and third neighbor hops take electrons from one site to another on the same sublattice, hence virtual double occupancy is excluded by the Pauli exclusion principle. The expectation value for the zero temperature staggered moment coming from the spin only Hamiltonian is thus scaled by the same $(1 - 8t^2/U)$ factor as in the case where $t' = t'' = 0$ ³³. The relevance of this term can be estimated by comparing theoretical and experimental estimates of the total magnetic moment. Here, we also find good agreement between the estimates of Lee *et al* in Ref. [44] and our calculated value. The charge renormalization is important here, as it scales the magnetization obtained by considering solely transverse spin fluctuations, by an amount clearly in excess of the experimental error bars. The comparison with experiment therefore provides an implicit illustration of its

importance in the real material.

Our results also bear on the question of the appropriate ratio of the bandwidth $\simeq 8t$ to the interaction strength U . First, note that on purely theoretical grounds, when U is of the order of the tight-binding band width, one expects the Hubbard model to undergo an insulator to metal transition, resulting in a breakdown of the perturbation expansion in t/U ^{57,68}. In our calculations, since the next order terms in the expansion of t/U is smaller than the leading term, there is no evidence of such a breakdown. In fact, for the value $t/U \simeq 0.126$ (or $U \simeq 8t$) that we found, we argue that the Hubbard model is definitely in the Mott insulator regime, as is necessary for the expansion to be valid. Indeed, at $t' = t'' = 0$, one can extract from quantum Monte Carlo calculations⁵⁶ that the Mott gap should close around $t/U \simeq 0.167$ (or $U \simeq 6t$), a value consistent with recent estimates from quantum cluster calculations^{14,15}. Although the critical t/U in general depends on t' ,^{57,58} for $t' = -0.3t$ on the square lattice, the critical t/U is still very close to the value appropriate for $t' = 0$ ⁶⁹. One can also check that for $t/U \simeq 0.126$, the single-particle spectral weight displays bands associated with antiferromagnetic excitations that disperse with J and are distinct from Hubbard bands further away from the Fermi energy.⁷⁰ When the gap is induced purely antiferromagnetic fluctuations (Slater mechanism), the distinct Hubbard bands are absent.¹¹ In addition, for insulating behavior induced by antiferromagnetic fluctuations, the potential energy decreases when insulating behavior occurs.⁷¹ This is not observed for $t/U \simeq 0.126$.⁷²

For $t' = t'' = 0$, the best fit value of $t/U \simeq 0.14$ found by Coldea *et al.*⁶ places La_2CuO_4 dangerously close to the insulator to metal transition discussed above. However, with the inclusion of t' and t'' and of all ring exchange terms to order $1/U^3$, we find a ratio $t/U \simeq 0.126$ which is decreased compared with the initial fit of Coldea *et al.*, which did not include these further neighbor hoppings. This places the ratio t/U for La_2CuO_4 within the Mott insulating phase of the Hubbard model discussed in the previous paragraph, by contrast with the result found in Ref. 12. If we had obtained the opposite result, namely that the best fit for t/U increases in the presence of t' and t'' , the whole approach would have become extremely doubtful as a description of La_2CuO_4 . Another approach, starting for example from the three-band model⁶⁸, would have become necessary. Instead, the result that we find here for t/U gives a consistent picture where the parameters of the one-band Hubbard model describe an insulator at half-filling. These parameters are also in agreement with those describing the doped insulator²⁵, including the sign and magnitude of the ratio t'/t'' . In fact, a non-vanishing t'' is necessary to obtain a consistent picture since, without it, t/U would increase⁵⁵ compared with its $t' = t'' = 0$ value, an undesirable state of affairs, as argued above.

To close, and reiterate, one of the noteworthy results of this work is that the presence of the ring exchange terms

	$4 \frac{t'^2 t^2}{U^3} \mathbf{S}_i \cdot \mathbf{S}_k \{ \epsilon_i \epsilon_j \epsilon_k \}$		$80 \frac{t'^2 t'^2}{U^3} \epsilon_i \epsilon_j \epsilon_l \epsilon_k P_1^{i,j,k,l}$
	$80 \frac{t'^2 t^2}{U^3} \epsilon_i \epsilon_j \epsilon_k \epsilon_l P_1^{i,j,k,l}$		$4 \frac{t'^2 t'^2}{U^3} \epsilon_i \epsilon_j \epsilon_l \epsilon_k (-1) P_2^{i,j,k,l}$
	$4 \frac{t'^2 t^2}{U^3} \epsilon_i \epsilon_j \epsilon_k \epsilon_l (-1) P_2^{i,j,k,l}$		$4 \frac{t'^2 t'^2}{U^3} \mathbf{S}_i \cdot \mathbf{S}_n \{ \epsilon_i \epsilon_j \epsilon_n \}$
	$4 \frac{t'^2 t^2}{U^3} \mathbf{S}_i \cdot \mathbf{S}_n \{ \epsilon_i \epsilon_j \epsilon_n \}$		$160 \frac{t'^2 t'^2}{U^3} \epsilon_i \epsilon_j \epsilon_l \epsilon_k \{ (\mathbf{S}_i \cdot \mathbf{S}_k) (\mathbf{S}_j \cdot \mathbf{S}_l) \}$ $+ 80 \frac{t'^4}{U^3} \epsilon_i \epsilon_j \epsilon_l \epsilon_k P_1^{i,j,k,l}$
	$80 \frac{t'^2 t^2}{U^3} \epsilon_i \epsilon_j \epsilon_m \epsilon_n P_1^{i,j,m,n}$		$4 \frac{t'^2 t'^2}{U^3} \epsilon_i \epsilon_j \epsilon_l \epsilon_k (-1) P_2^{i,j,k,l}$
	$4 \frac{t'^2 t^2}{U^3} \epsilon_i \epsilon_j \epsilon_m \epsilon_n (-1) P_2^{i,j,m,n}$		$4 \frac{t'^2 t'^2}{U^3} \epsilon_i \epsilon_j \epsilon_k \{ \vec{S}_i \cdot \vec{S}_k + \vec{S}_j \cdot \vec{S}_l \}$
	$80 \frac{t^2}{U^3} t' t'' \epsilon_i \epsilon_j \epsilon_m \epsilon_n P_1^{i,j,n,m}$		$4 \frac{t'^2 t'^2}{U^3} \epsilon_i \epsilon_j \epsilon_k \{ \vec{S}_i \cdot \vec{S}_k \}$
	$4 \frac{t^2}{U^3} t' t'' \epsilon_i \epsilon_j \epsilon_m \epsilon_n (-1) P_2^{i,j,n,m}$		$80 \frac{t'^4}{U^3} \epsilon_i \epsilon_j \epsilon_k \epsilon_l P_1^{i,j,k,l}$
	$80 \frac{t^2 t' t''}{U^3} \epsilon_i \epsilon_j \epsilon_m \epsilon_k P_1^{i,j,k,m}$		$4 \frac{t'^4}{U^3} \epsilon_i \epsilon_j \epsilon_k \epsilon_l P_2^{i,j,k,l}$
	$80 \frac{t^2 t' t''}{U^3} \epsilon_i \epsilon_j \epsilon_m \epsilon_k P_1^{i,j,k,m}$		$80 \frac{t^2 t'^2}{U^3} \epsilon_i \epsilon_j \epsilon_k \epsilon_l P_1^{i,j,k,l}$
	$4 \frac{t^2 t' t''}{U^3} \epsilon_i \epsilon_j \epsilon_k \epsilon_l (-1) P_2^{i,j,k,l}$		$4 \frac{t^2 t'^2}{U^3} \epsilon_i \epsilon_j \epsilon_k \epsilon_l P_2^{i,j,k,l}$

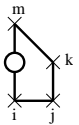
APPENDIX B: MEAN-FIELD SOLUTION OF SPIN HAMILTONIAN WITH t , t' AND t''

The purpose of this appendix is to determine the sublattice magnetization at zero temperature for the $t - t' - t'' - U$ Hubbard model using the Hartree-Fock (mean-field) method of Ref. [59]. From Eqs. (17,18), the $t - t' - t'' - U$ Hubbard model is:

$$H_H = T + T' + T'' + V \quad (\text{B1})$$

$$= -t \sum_{i,j_1;\sigma} c_{i,\sigma}^\dagger c_{j_1,\sigma} - t' \sum_{i,j_2;\sigma} c_{i,\sigma}^\dagger c_{j_2,\sigma} - t'' \sum_{i,j_3;\sigma} c_{i,\sigma}^\dagger c_{j_3,\sigma} + U \sum_i n_{i,\uparrow} n_{i,\downarrow}, \quad (\text{B2})$$

where j_1 , j_2 and j_3 are respectively the first, second and third nearest neighbors of i . Fourier transforming this



$$4 \frac{t^2 t' t''}{U^3} \epsilon_i \epsilon_j \epsilon_m \epsilon_k (-1) P_2^{i,j,k,m}$$

expression leads to:

$$H_H = \sum_{\mathbf{k}, \sigma} (\epsilon_{\mathbf{k}} + \epsilon'_{\mathbf{k}} + \epsilon''_{\mathbf{k}}) c_{\mathbf{k}, \sigma}^\dagger c_{\mathbf{k}, \sigma} + \frac{U}{2N} \sum_{\mathbf{k}, \mathbf{k}', \mathbf{q}} \sum_{\sigma, \sigma', \beta, \beta'} \delta_{\sigma, \sigma'} \delta_{\beta, \beta'} c_{\mathbf{k}', \sigma}^\dagger c_{-\mathbf{k}'+\mathbf{q}, \beta'} c_{-\mathbf{k}+\mathbf{q}, \beta} c_{\mathbf{k}, \sigma}, \quad (\text{B3})$$

where:

$$\begin{cases} \epsilon_{\mathbf{k}} = -2t(\cos(k_x) + \cos(k_y)), \\ \epsilon'_{\mathbf{k}} = -2t'(\cos(k_x + k_y) + \cos(k_x - k_y)), \\ \epsilon''_{\mathbf{k}} = -2t''(\cos(2k_x) + \cos(2k_y)). \end{cases} \quad (\text{B4})$$

The sublattice magnetization for nesting wave vector \mathbf{Q} is defined by:

$$M = \langle \Omega | S_{\mathbf{Q}}^z | \Omega \rangle, \quad (\text{B5})$$

where we consider the case where the magnetization is polarized along the \hat{z} direction. $|\Omega\rangle$ is the spin density wave ground state and \mathbf{Q} . The spin density operator $S_{\mathbf{q}}^i$ for arbitrary \mathbf{q} wave vector is defined by:

$$S_{\mathbf{q}}^i = \frac{1}{N} \sum_{\mathbf{k}, \alpha, \beta} c_{\mathbf{k}+\mathbf{q}, \alpha}^\dagger \hat{\sigma}_{\alpha, \beta}^i c_{\mathbf{k}, \beta}, \quad (\text{B6})$$

N being the number of sites.

We define new operators $\gamma_{\mathbf{k}, \alpha}^c$ and $\gamma_{\mathbf{k}, \alpha}^v$ through the Bogoliubov transformation:

$$\left\{ \begin{array}{l} \gamma_{\mathbf{k}, \alpha}^c = u_{\mathbf{k}} c_{\mathbf{k}, \alpha} + v_{\mathbf{k}} \sum_{\beta} \hat{\sigma}_{\alpha, \beta}^3 c_{\mathbf{k}+\mathbf{Q}, \beta}, \\ \gamma_{\mathbf{k}, \alpha}^v = v_{\mathbf{k}} c_{\mathbf{k}, \alpha} - u_{\mathbf{k}} \sum_{\beta} \hat{\sigma}_{\alpha, \beta}^3 c_{\mathbf{k}+\mathbf{Q}, \beta}. \end{array} \right\}, \quad (\text{B7})$$

and inject (B7) into the Hartree-Fock factorization⁵⁹ of Hamiltonian (B3), finding:

$$E_{\mathbf{k}} = \epsilon'_{\mathbf{k}} + \epsilon''_{\mathbf{k}} \pm \sqrt{\Delta^2 + \epsilon_{\mathbf{k}}^2}, \quad (\text{B8})$$

where the density wave gap Δ is given by:

$$\Delta = -\frac{UM}{2}. \quad (\text{B9})$$

The Bogoliubov coefficients for this transformation $u_{\mathbf{k}}$ and $v_{\mathbf{k}}$ are:

$$\left\{ \begin{array}{l} u_{\mathbf{k}}^2 = \frac{1}{2} \left(1 + \frac{\epsilon_{\mathbf{k}}}{E_{\mathbf{k}} - \epsilon'_{\mathbf{k}} - \epsilon''_{\mathbf{k}}} \right), \\ v_{\mathbf{k}}^2 = \frac{1}{2} \left(1 - \frac{\epsilon_{\mathbf{k}}}{E_{\mathbf{k}} - \epsilon'_{\mathbf{k}} - \epsilon''_{\mathbf{k}}} \right), \end{array} \right. \quad (\text{B10})$$

With the valence band filled and the conduction band empty, since the calculation here is done at zero temperature, it follows from the above relationships that

$$M = \langle \Omega | S_{\mathbf{Q}}^z | \Omega \rangle = \frac{2}{N} \sum_{\mathbf{k}} u_{\mathbf{k}} v_{\mathbf{k}}; \quad (\text{B11})$$

hence:

$$M = -\frac{4}{N} \sum_{\mathbf{k}} \frac{\Delta}{E_{\mathbf{k}} - \epsilon'_{\mathbf{k}} - \epsilon''_{\mathbf{k}}}. \quad (\text{B12})$$

Putting (B9) into (B12) gives the following self-consistent equation for the sublattice magnetization:

$$\frac{1}{U} = \frac{1}{N} \sum_{\mathbf{k}} \frac{1}{\sqrt{\epsilon_{\mathbf{k}}^2 + \left(\frac{UM}{2}\right)^2}}. \quad (\text{B13})$$

We remark that equation (B13) is independent of $\epsilon'_{\mathbf{k}}$ or $\epsilon''_{\mathbf{k}}$. Considering $t/U \ll 1$, we can expand the square roots of (B13) in $\epsilon_{\mathbf{k}}/U$, after which we find:

$$\frac{1}{N} \sum_{\mathbf{k}} \frac{1}{(\epsilon_{\mathbf{k}}^2 + \Delta^2)^{1/2}} = \frac{1}{N} \sum_{\mathbf{k}} \frac{2}{UM} \left(1 - \frac{2\epsilon_{\mathbf{k}}^2}{U^2 M^2} \right) = \frac{1}{U}. \quad (\text{B14})$$

Further simplifications lead to:

$$M = 1 - \frac{4}{NM^2} \sum_{\mathbf{k}} \frac{\epsilon_{\mathbf{k}}^2}{U^2}. \quad (\text{B15})$$

To first order in t/U we obtain:

$$M \approx 1 - \frac{4}{N} \sum_{\mathbf{k}} \frac{\epsilon_{\mathbf{k}}^2}{U^2}. \quad (\text{B16})$$

Since $\frac{1}{N} \sum_{\mathbf{k}} \frac{\epsilon_{\mathbf{k}}^2}{U^2} = \frac{4t^2}{U^2} \frac{1}{N} \sum_{\mathbf{k}} (\cos(k_x) + \cos(k_y))^2$, and

$$\frac{1}{N} \sum_{\mathbf{k}} (\cos(k_x) + \cos(k_y))^2 = \frac{1}{2}, \quad (\text{B17})$$

we

conclude that:

$$M = 1 - 8 \frac{t^2}{U^2}. \quad (\text{B18})$$

This result is equivalent to that obtained through the unitary transformation method in Eq. (53) if transverse spin fluctuations are neglected, as they are in the Hartree-Fock approach. Mathematically, it is the property $\epsilon_{\mathbf{k}} = -\epsilon_{\mathbf{k}+\mathbf{Q}}$ that makes nearest-neighbor hopping different from the other two hops which both obey, instead, $\epsilon'_{\mathbf{k}} = \epsilon'_{\mathbf{k}+\mathbf{Q}}$, $\epsilon''_{\mathbf{k}} = \epsilon''_{\mathbf{k}+\mathbf{Q}}$. Note that $\epsilon_{\mathbf{k}}$, $\epsilon'_{\mathbf{k}}$, $\epsilon''_{\mathbf{k}}$ in this appendix are the quasi-particle energies, which should not be confused with the spin-wave (magnon) energies in Section III A 1.

Physically, since t' and t'' are hops within the same sublattice (parallel spins) of the classical Néel antiferromagnetic solution, in the strong coupling limit the Pauli principle prohibits hopping between these sites. Hence, to leading order, t' and t'' cannot change double occupancy or, in other words, produce charge fluctuations (or ‘‘charge renormalization’’).

APPENDIX C: SPIN WAVE RESULTS

By introducing the transformations of Eq. (24) in $H_{s,\text{quad}}^{(4)}(t, t', t'', U)$ (equation (23)), passing into Fourier

space, and collecting all terms, we obtain, after some tedious but straightforward algebra, the following expressions for the functions $A_{\mathbf{k}}$ and $B_{\mathbf{k}}$:

$$\begin{aligned}
\frac{U}{(4t^2)}A_{\mathbf{k}} = & 4J_1S + J_2S \left[4 \cos(k_x) \cos(k_y) - 4 \right] + J_3S \left[2 \cos(2k_x) + 2 \cos(2k_y) - 4 \right] \\
& - J_c S^3 \left[4 + 4 \cos(k_x) \cos(k_y) \right] \\
& + 40S^3 \left(\frac{t}{U} \right)^2 \left(\frac{t'}{t} \right)^2 \left[-4 + 2 \cos(k_x + k_y) + 2 \cos(k_x - k_y) \right] + 16S \left(\frac{t}{U} \right)^2 \left(\frac{t'}{t} \right)^2 \\
& + 20S^3 \left(\frac{t}{U} \right)^2 \left(\frac{t'}{t} \right)^2 \left[16 - 16 \cos(k_x) \cos(k_y) + 4 \cos(2k_x) + 4 \cos(2k_y) \right] \\
& - S \left(\frac{t}{U} \right)^2 \left(\frac{t'}{t} \right)^2 \left[8(\cos(k_x) \cos(k_y) - 1) + 4(\cos(2k_x) + \cos(2k_y)) + 16 + 8(\cos(k_x) \cos(k_y) - 1) \right] \\
& + 12S \left(\frac{t}{U} \right)^2 \left(\frac{t'}{t} \right)^2 \\
& + 20S^3 \left(\frac{t}{U} \right)^2 \left(\frac{t'}{t} \right)^2 \left[-16 + 8 \cos(2k_x) + 8 \cos(2k_y) \right] \\
& - S \left(\frac{t}{U} \right)^2 \left(\frac{t''}{t} \right)^2 \left[32 + 8(\cos(2k_x) + \cos(2k_y) - 2) \right] \\
& - 20S^3 \left(\frac{t}{U} \right)^2 \left(\frac{t'}{t} \right) \left(\frac{t''}{t} \right) \left[32 - 8(\cos(2k_x) + \cos(k_x - k_y) + \cos(k_x + k_y) + \cos(2k_y)) \right] \\
& - \left(\frac{t}{U} \right)^2 \left(\frac{t'}{t} \right) \left(\frac{t''}{t} \right) S \left[32 + 16(\cos(k_x) \cos(k_y)) + 8(\cos(2k_x) + \cos(2k_y)) \right] \\
& + 20 \left(\frac{t}{U} \right)^2 \left(\frac{t'}{t} \right) \left(\frac{t''}{t} \right) S^3 \left[16 - (16(\cos(k_x) \cos(k_y) - 1)) - 8(\cos(2k_x) + \cos(2k_y) - 2) \right. \\
& \quad \left. + 4(4 \cos(k_x) \cos(k_y) - 4) \right] \\
& - 2 \left(\frac{t}{U} \right)^2 \left(\frac{t'}{t} \right) \left(\frac{t''}{t} \right) S \left[8 \cos(k_x) \cos(k_y) + 4 \cos(2k_x) + 4 \cos(2k_y) \right] \\
& + 20S^3 \left(\frac{t}{U} \right)^2 \left(\frac{t'}{t} \right)^2 \left(\frac{t''}{t} \right)^2 \left[-32 + 16(\cos(2k_x) + \cos(2k_y)) + 16 \cos(k_x) \cos(k_y) \right. \\
& \quad \left. - 8 \cos(2k_x + 2k_y) - 8 \cos(2k_x - 2k_y) \right] \\
& + 2S \left(\frac{t}{U} \right)^2 \left(\frac{t'}{t} \right)^2 \left(\frac{t''}{t} \right)^2 \left[-48 + 8(\cos(2k_x) + \cos(2k_y)) + 24(\cos(k_x) \cos(k_y)) \right. \\
& \quad \left. + 4(\cos(2k_x + 2k_y) + \cos(2k_x - 2k_y)) \right] \\
& + S \left(\frac{t}{U} \right)^2 \left(\frac{t'}{t} \right)^2 \left(\frac{t''}{t} \right)^2 \left[32 \cos(k_x) \cos(k_y) - 32 \right] \\
& + S \left(\frac{t}{U} \right)^2 \left(\frac{t'}{t} \right)^2 \left(\frac{t''}{t} \right)^2 \left[-16 + 4(\cos(3k_x + k_y) + \cos(3k_x - k_y) + \cos(k_x + 3k_y) + \cos(k_x - 3k_y)) \right] \\
& + 20S^3 \left(\frac{t}{U} \right)^2 \left(\frac{t''}{t} \right)^4 \left[-4 + 4(\cos(2k_x) + \cos(2k_y)) - 2 \cos(2k_x + 2k_y) - 2 \cos(2k_x - 2k_y) \right] \\
& + S \left(\frac{t}{U} \right)^2 \left(\frac{t''}{t} \right)^4 \left[(4 \cos(2k_x) + 4 \cos(2k_y)) - 12 + 2 \cos((2k_x + 2k_y) + \cos(2k_x - 2k_y)) \right] \\
& + 40S^3 \left(\frac{t'}{t} \right)^2 \left(\frac{t}{U} \right)^2 \left[16(\cos(k_x) \cos(k_y) - 1) \right] \\
& + 2S \left(\frac{t'}{t} \right)^2 \left(\frac{t}{U} \right)^2 \left[16 + 16 \cos(k_x) \cos(k_y) \right]
\end{aligned}$$

(C1)

$$\begin{aligned}
\frac{U}{(4t^2)}B_{\mathbf{k}} = & 2J_1S \left[\cos(k_x) + \cos(k_y) \right] - 4J_cS^3 \left[\cos(k_x) + \cos(k_y) \right] \\
& + S \left(\frac{t}{U} \right)^2 \left(\frac{t'}{t} \right)^2 4 \left[\cos(2k_x + k_y) + \cos(2k_y + k_x) + \cos(2k_x - k_y) + \cos(2k_y - k_x) \right] \\
& + 80S^3 \left(\frac{t}{U} \right)^2 \left(\frac{t'}{t} \right)^2 \left[\cos(k_x) + \cos(k_y) \right] \\
& - S \left(\frac{t}{U} \right)^2 \left(\frac{t'}{t} \right)^2 \left[4(\cos(k_x) + \cos(k_y)) + 4(\cos(k_x) + \cos(k_y)) + 4(\cos(k_x) + \cos(k_y)) \right] \\
& + S \left(\frac{t}{U} \right)^2 \left(\frac{t''}{t} \right)^2 \left[2(\cos(3k_x) + \cos(3k_y)) + 2 \cos(2k_x + k_y) + 2 \cos(2k_x - k_y) \right. \\
& \quad \left. + 2 \cos(k_x + 2k_y) + 2 \cos(k_x - 2k_y) \right] \\
& + 20S^3 \left(\frac{t}{U} \right)^2 \left(\frac{t''}{t} \right)^2 \left[-8(\cos(k_x) + \cos(k_y)) \right. \\
& \quad \left. + 4(\cos(2k_x + k_y) + \cos(2k_x - k_y) + \cos(k_x + 2k_y) + \cos(k_x - 2k_y)) \right] \\
& - S \left(\frac{t}{U} \right)^2 \left(\frac{t''}{t} \right)^2 \left[8(\cos(k_x) + \cos(k_y)) + 4(\cos(2k_x + k_y) + \cos(2k_x - k_y)) \right. \\
& \quad \left. + \cos(k_x + 2k_y) + \cos(k_x - 2k_y) \right] \\
& - 20S^3 \left(\frac{t}{U} \right)^2 \left(\frac{t'}{t} \right) \left(\frac{t''}{t} \right) \left[4(2 \cos(k_x) + 2 \cos(k_y)) - 4(\cos(2k_x + k_y) + \cos(2k_x - k_y)) \right. \\
& \quad \left. + \cos(2k_y + k_x) + \cos(2k_y - k_x) \right] \\
& - S \left(\frac{t}{U} \right)^2 \left(\frac{t'}{t} \right) \left(\frac{t''}{t} \right) \left[24(\cos(k_x) + \cos(k_y)) + 4(\cos(2k_x + k_y) + \cos(2k_x - k_y)) \right. \\
& \quad \left. + \cos(2k_y + k_x) + \cos(2k_y - k_x) \right] \\
& + 20S^3 \left(\frac{t}{U} \right)^2 \left(\frac{t'}{t} \right) \left(\frac{t''}{t} \right) \left[8(\cos(k_x) + \cos(k_y)) + 8(\cos(k_x) + \cos(k_y)) - 4(\cos(2k_x + k_y)) \right. \\
& \quad \left. + \cos(2k_x - k_y) + \cos(k_x + 2k_y) + \cos(k_x - 2k_y) \right] \\
& - 2S \left(\frac{t}{U} \right)^2 \left(\frac{t'}{t} \right) \left(\frac{t''}{t} \right) \left[4 \cos(k_x) + 4 \cos(k_y) + 2(\cos(2k_x + k_y) + \cos(2k_x - k_y)) \right. \\
& \quad \left. + \cos(k_x - 2k_y) + \cos(k_x + 2k_y) \right] \\
& + 40S^3 \left(\frac{t}{U} \right)^2 \left(\frac{t'}{t} \right)^2 \left[-8(\cos(k_x) + \cos(k_y)) + (2 \cos(2k_x - k_y) + 2 \cos(2k_x + k_y) + 2 \cos(k_x + 2k_y)) \right. \\
& \quad \left. + 2 \cos(k_x - 2k_y) + 4(\cos(k_x) + \cos(k_y)) \right] \\
& + 2S \left(\frac{t}{U} \right)^2 \left(\frac{t'}{t} \right)^2 \left[12(\cos(k_x) + \cos(k_y)) + (2 \cos(2k_x - k_y) + 2 \cos(2k_x + k_y) + 2 \cos(k_x + 2k_y)) \right. \\
& \quad \left. + 2 \cos(k_x - 2k_y) \right]
\end{aligned} \tag{C2}$$

**APPENDIX D: SPIN WAVE
RENORMALIZATION FACTOR Z_c**

We consider the terms in the transformed spin only Hamiltonian of order $1/S^2$ as a perturbation to the lowest order spin wave Hamiltonian. Within this framework the perturbation gives quartic terms in boson creation and annihilation operators, for which we have to diagonalize the set of 2×2 matrices of elements $\langle 0 | \gamma_{\mathbf{k}} H_4 \gamma_{\mathbf{k}}^\dagger | 0 \rangle$, where $(\gamma_{\mathbf{k}}, \gamma'_{\mathbf{k}}) \in \{\alpha_{\mathbf{k}}, \beta_{\mathbf{k}}\}$.

We first review the situation when t' and t'' are set equal to zero:

$$\begin{cases} H_2(t) = SJ_1(t) \sum_{\langle i,j \rangle} (a_i^\dagger a_i + b_j^\dagger b_j) + 2(a_i b_j + a_i^\dagger b_j^\dagger), \\ H_4(t) = -\frac{J_1(t)}{2} \sum_{\langle i,j \rangle} (a_i^\dagger a_i a_i b_j + a_i b_j^\dagger b_j b_j + a_i^\dagger a_i^\dagger a_i b_j^\dagger \\ + a_i^\dagger b_j^\dagger b_j^\dagger b_j) + 2a_i^\dagger a_i b_j^\dagger b_j. \end{cases} \quad (\text{D1})$$

Here, we work to leading order in t/U , for which $J_1(t) = 4t^2/U$. Note that, within this appendix, we use a compact notation: $H_{s,\text{quad}}^{(4)} \rightarrow H_2$ and $H_{s,\text{quart}}^{(4)} \rightarrow H_4$. It turns out that the 2×2 perturbation matrix is proportional to the identity matrix. We find:

$$\begin{aligned} \delta\epsilon_{\mathbf{k}} = \frac{1}{2N} J_1(t) \left[\right. \\ -2(u_{\mathbf{k}}^2 + v_{\mathbf{k}}^2) \sum_{\mathbf{k}'} (u_{\mathbf{k}'} v_{\mathbf{k}'} (2 \cos(k'_x) + 2 \cos(k'_y))) \\ - (u_{\mathbf{k}} v_{\mathbf{k}} (2 \cos(k_x) + 2 \cos(k_y))) \sum_{\mathbf{k}'} 2v_{\mathbf{k}'}^2 \\ + 4(u_{\mathbf{k}}^2 + v_{\mathbf{k}}^2) \sum_{\mathbf{k}'} 2v_{\mathbf{k}'}^2 \\ \left. + 4u_{\mathbf{k}} v_{\mathbf{k}} \sum_{\mathbf{k}'} u_{\mathbf{k}'} v_{\mathbf{k}'} (2 \cos(k_x - k'_x) + 2 \cos(k_y k'_y)) \right], \end{aligned} \quad (\text{D2})$$

from which the magnon energy correction $\Delta_{\mathbf{k}} \equiv \Delta\epsilon_{\mathbf{k}}/\epsilon_{\mathbf{k}}$ can be computed. $\Delta_{\mathbf{k}}$ converges numerically to give

$$\Delta_{\mathbf{k}} \simeq 0.1579, \quad (\text{D3})$$

uniformly over the Brillouin zone, as found previously in Ref. [43].

When t' or t'' are brought into the picture the leading effects are to create second and third nearest neighbor interactions $J_2(t') = 4(t')^2/U$ and $J_3(t'') = 4(t'')^2/U$ producing new contributions to the quartic Hamiltonian:

$$\begin{cases} H_4(t') = J_2(t') \sum_{\langle\langle i,j \rangle\rangle} a_i^\dagger a_i a_j^\dagger a_j - \frac{1}{4} \left[a_i^\dagger a_i a_i a_j^\dagger \right. \\ \left. + a_i^\dagger a_j^\dagger a_j^\dagger a_j + a_i^\dagger a_i^\dagger a_i a_j + a_i^\dagger a_j^\dagger a_j a_j \right] \\ H_4(t'') = J_3(t'') \sum_{\langle\langle\langle i,j \rangle\rangle\rangle} a_i^\dagger a_i a_j^\dagger a_j - \frac{1}{4} \left[a_i^\dagger a_i a_i a_j^\dagger \right. \\ \left. + a_i^\dagger a_j^\dagger a_j^\dagger a_j + a_i^\dagger a_i^\dagger a_i a_j + a_i^\dagger a_j^\dagger a_j a_j \right] \end{cases} \quad (\text{D4})$$

The contribution coming from t' reads:

$$\begin{aligned} \delta\epsilon'_{\mathbf{k}} = \frac{1}{2N} J_2(t') \left[2(u_{\mathbf{k}}^2 + v_{\mathbf{k}}^2) \sum_{\mathbf{k}'} 4v_{\mathbf{k}'}^2 \right. \\ + (u_{\mathbf{k}}^2 + v_{\mathbf{k}}^2) \sum_{\mathbf{k}'} 2(u_{\mathbf{k}'}^2 + v_{\mathbf{k}'}^2) \times \\ \left(2 \cos((k_x + k_y) - (k'_x + k'_y)) + \right. \\ \left. 2 \cos((k_x - k_y) - (k'_x - k'_y)) \right) \\ + (u_{\mathbf{k}}^2 + v_{\mathbf{k}}^2) \sum_{\mathbf{k}'} (u_{\mathbf{k}'}^2 + v_{\mathbf{k}'}^2) \times \\ 2 \left(\cos(k'_x + k'_y) + \cos(k'_x - k'_y) \right) \\ \left. + 2(\cos(k_x + k_y) + \cos(k_x - k_y)) \times \right. \\ \left. \sum_{\mathbf{k}'} (u_{\mathbf{k}'}^2 + v_{\mathbf{k}'}^2) 2v_{\mathbf{k}'}^2 \right] \end{aligned}, \quad (\text{D5})$$

while that from t'' reads:

$$\begin{aligned} \delta\epsilon''_{\mathbf{k}} = \frac{1}{2N} J_3(t'') \left[2(u_{\mathbf{k}}^2 + v_{\mathbf{k}}^2) \sum_{\mathbf{k}'} 4v_{\mathbf{k}'}^2 \right. \\ + (u_{\mathbf{k}}^2 + v_{\mathbf{k}}^2) \sum_{\mathbf{k}'} 2(u_{\mathbf{k}'}^2 + v_{\mathbf{k}'}^2) \left(2 \cos(2k_x - 2k'_x) \right. \\ \left. + 2 \cos(2k_y - 2k'_y) \right) \\ + (u_{\mathbf{k}}^2 + v_{\mathbf{k}}^2) \sum_{\mathbf{k}'} (u_{\mathbf{k}'}^2 + v_{\mathbf{k}'}^2) 2 \left(\cos(2k'_x) + \cos(2k'_y) \right) \\ \left. + 2 \left(\cos(2k_x) + \cos(2k_y) \right) \sum_{\mathbf{k}'} (u_{\mathbf{k}'}^2 + v_{\mathbf{k}'}^2) 2v_{\mathbf{k}'}^2 \right] \end{aligned} \quad (\text{D6})$$

We now find that the total contribution of the terms coming from t , t' and t'' is no longer independent of wave vector, but the two-fold degeneracy for each \mathbf{k} remains. The evolution of $Z_c(\mathbf{k})$ over the Brillouin zone is shown in Fig. 2 for the parameter set (38).

Dividing the contributions to $Z_c(\mathbf{k})$ into three parts coming from t , t' and t'' and denoting an average over the Brillouin zone by $\langle \cdot \rangle_{\mathbf{k}}$ we find

$$\begin{cases} \langle \Delta_{\mathbf{k}} \rangle = 0.187, \\ \langle \Delta'_{\mathbf{k}} \rangle = 0.019, \\ \langle \Delta''_{\mathbf{k}} \rangle = 0.013, \end{cases} \quad (\text{D7})$$

using the parameter set (38). Note that here $\Delta'_{\mathbf{k}}$ and $\Delta''_{\mathbf{k}}$ do not factorize analytically in Eq. (D5) or (D6), rather, for each wave vector, we calculate $\Delta'_{\mathbf{k}} \equiv \delta\epsilon'_{\mathbf{k}}/\epsilon'_{\mathbf{k}}$ and similarly for $\Delta''_{\mathbf{k}}$. Note also that as t' and t'' become non-zero, even the first term evolves. This is because $\epsilon_{\mathbf{k}}$ is itself a function of t' and t'' and so it changes as these parameters are switched on.

As discussed in Section III A 4, incorporating the \mathbf{k} -dependence of $Z_c(\mathbf{k})$ makes the fitting procedure somewhat computationally cumbersome and slow from a CPU speed point of view. There are two reasons for this. Firstly, it is due to the need to constantly redo the ‘‘internal’’ sum over \mathbf{k}' in Eqs. (D2), (D5) and (D6) whenever the t , t' , t'' and U parameters are readjusted. Secondly,

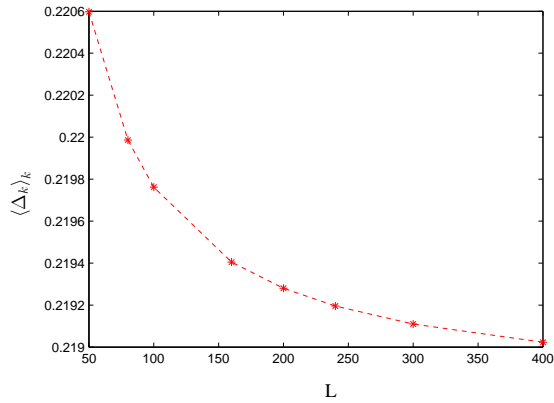


FIG. 7: (Color online) Evolution of $\langle \Delta_k \rangle_k$ as a function of the number of points in the Brillouin zone

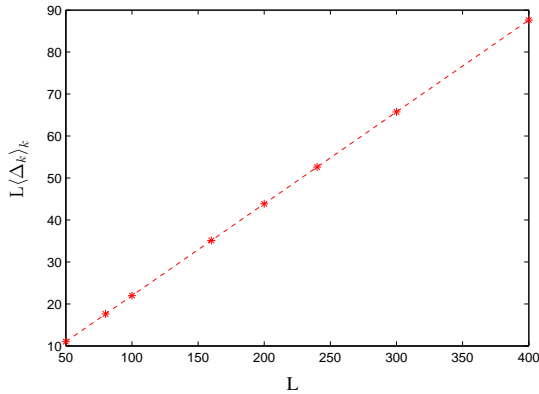


FIG. 8: (Color online) Evolution of $L \times \langle \Delta_k \rangle_k$ as a function of the number of points in the Brillouin zone.

to compound this problem the CPU time is further increased by noting that the sums over \mathbf{k}' in Eqs. (D2), (D5) and (D6) converge somewhat slowly with system size. \mathbf{k}' in equations (D2,D5,D6) This is illustrated in Fig. 7, for a magnetic Brillouin zone of linear dimension L , for the parameter set (38) (here the lattice parameter is taken to be unity) Re-plotting the data in Fig. 8, we show that $\langle \Delta_k \rangle_k$ scales with system size as

$$\langle \Delta_k \rangle_k(L) = \frac{\alpha}{L} + \langle \Delta_k \rangle_k(\infty), \quad (\text{D8})$$

where α is a constant, from which we find:

$$\langle \Delta_k \rangle_k(\infty) \simeq 0.219. \quad (\text{D9})$$

The width of the dispersion of $\Delta(\mathbf{k})$ over the Brillouin zone, $\sigma(\Delta(\mathbf{k}))$, scales in a similar way and we eventually find

$$\frac{\sigma(\Delta_k)}{\langle \Delta_k \rangle_k}(\infty) \simeq 0.33 \times 10^{-3}. \quad (\text{D10})$$

Finite size effects lead to negligible corrections compared to the least squares fitting procedure, for $L \sim 100$. A magnetic Brillouin zone of this size was used to make the fits described in the main text.

APPENDIX E: PARTIALLY CONSTRAINED SPIN-WAVE FITS

For a number of compounds, such as $\text{Sr}_2\text{CuO}_2\text{Cl}_2$, $\text{Bi}_2\text{Sr}_2\text{CaCu}_2\text{O}_{8+\delta}$ (BSCCO, Bi-2212) and $\text{YBa}_2\text{Cu}_3\text{O}_{6+\delta}$ (YBCO), values of $t' \sim -0.3$ eV, $t'' \sim 0.2$ eV, and $U > 10$ eV are commonly used²². However, these values are not truly universal among the cuprates. For example, in Ref. [25], local density approximation (LDA) calculations do predict variations from one compound to the other. In particular, for La_2CuO_4 , $t'/t = -0.17$ is obtained, and which corresponds to the value used in ARPES data analysis²¹.

A recent ARPES experiment by Yoshida *et al.*¹⁹ on *doped* $\text{La}_{2-x}\text{Sr}_x\text{CuO}_4$ finds that t' varies slightly between compositions. For $x = 0.03$, they obtain $t'/t \approx -0.2$ and $t''/t' \approx 0.5$. To the best of our knowledge, there exist no ARPES measurements on undoped La_2CuO_4 , but one may extrapolate to $t'/t = -0.21$ for this composition. In this context, we have performed a constrained fit to the spin-wave dispersion data of Ref. [6], imposing $t'/t = -0.2$, $t''/t' = 0.5$ and $t = 0.25$ eV and only allowing U to vary. We were unable to find a reasonable value of U with such constraints. Indeed, we found $U \sim 1.6$ eV with a poor quality of fit.

We then allowed *both* t and U to vary. The motivation being that the effective ratios $t'/t = -0.2$ and $t''/t' = 0.5$ could be well determined by ARPES, while the value of t determined from the electronic bandwidth could be strongly renormalized. The best fit then obtained was $t = 0.3430$ eV and $U = 2.55$ eV, hence $U/t = 7.42$. Compared to the fit with free t , t' , t'' and U values, the overall χ^2 , with

$$\chi^2 = \sum_n \frac{(E_n^{\text{experimental}} - E_n^{\text{fit}})^2}{(\text{experimental uncertainty})_n}, \quad (\text{E1})$$

where E_i is n 'the magnon energy data point, is increased by roughly 25% for the fit with t'/t and t''/t' constrained compared with the fit with the values in Eq. (38).

This value of $t \approx 0.34$ eV agrees roughly with those found by Coldea *et al.*⁶, and the value $U \approx 2.55$ is in-between that of Ref. [6 and the one found in this work and reported in Eq. (38). In other words, for the constrained values of t' and t'' used in such a fit, the values are sufficiently “small” that the results for $t' = t'' = 0$ of Ref. [6] are more or less recovered. In other words, the ratio t/U is a crucial parameter in the fit. Working with a fit with t'/t and t''/t' fully constrained leads to a (reduced) ratio t/U compared to the unconstrained fit of Eq. (38). Yet, this reduced $U = 2.55$ eV also gives a reduced $t = 0.34$ eV, with the result that while the unconstrained fit has $t/U = 0.126$, the constrained fit has $t/U = 0.34/2.55 = 0.133$ (I just calculated) and Coldea *et al.* finds $t/U = 0.135$. Given that t'/t'' is essentially the same in the constrained and unconstrained fits, one can think of the constrained fit as an intermediate point in switching on t' and t'' at constant t'/t'' . Indeed, we

find the following progression of values, moving from the Coldea *et al.* results, the constrained fit results and the unconstrained fit results: $U = 2.3$ eV, 2.55 eV and 3.34 eV, $t = 0.3$ eV, 0.34 eV and 0.42 eV, and $t/U = 0.135$, 0.133, and 0.126. This progression of parameters appears monotonous. Given that we expect t' and t'' to frustrate Néel ordering, we also expect the metal insu-

lator transition also to appear for smaller values of t/U with increasing t' and t'' . Our results are reassuring in this respect because we find the fitted t/U value getting progressively small as t' and t'' are turned on, consistent with the system remaining in the insulating Néel ordered state.

-
- ¹ P. W. Anderson, *Science* **235**, 1196 (1987).
² J. D. Reger and A. P. Young, *Phys. Rev. B* **37**, 5978 (1988).
³ J. E. Hirsch and S. Tang, *Phys. Rev. Lett.* **62**, 591 (1989).
⁴ G. Shirane, Y. Endoh, R. J. Birgeneau, M. A. Kastner, Y. Hidaka, M. Oda, M. Suzuki, and T. Murakami, *Phys. Rev. Lett.* **59**, 1613 (1987).
⁵ Y. Endoh, K. Yamada, R. J. Birgeneau, D. R. Gabbe, H. P. Jenssen, M. A. Kastner, C. J. Peters, P. J. Picone, T. R. Thurston, J. M. Tranquada, et al., *Phys. Rev. B* **37**, 7443 (1988).
⁶ R. Coldea, S. M. Hayden, G. Aeppli, T. G. Perring, C. D. Frost, T. E. Mason, S.-W. Cheong, and Z. Fisk, *Phys. Rev. Lett.* **86**, 5377 (2001).
⁷ H. M. Rønnow, D. F. McMorrow, R. Coldea, A. Harrison, I. D. Youngson, T. G. Perring, G. Aeppli, O. Syljuåsen, K. Lefmann, and C. Rischel, *Phys. Rev. Lett.* **87**, 037202 (2001).
⁸ P. Dirac, *The Principles of Quantum Mechanics* (Clarendon, Oxford, 1947).
⁹ P. Dirac, *Proc. Roy. Soc. Lond.* **123**, 714 (1929).
¹⁰ M. Roger, *J. Phys. Chem. Solids* **66**, 1412 (2005).
¹¹ Y. Vilk and A.-M. Tremblay, *J. Phys I (France)* **7**, 1309 (1997).
¹² A. Comanac, L. De' Medici, M. Capone, and A. J. Millis, *Nature Physics* **4**, 287 (2008).
¹³ Y. Zhang and M. Imada, *Phys. Rev. B* (2007).
¹⁴ H. Park, K. Haule, and G. Kotliar, arXiv:0803.1324 (2008).
¹⁵ E. Gull, P. Werner, M. Troyer, and A. Millis, *cond-mat/0805.3778* (2008).
¹⁶ M. Ferrero, P. Cornaglia, L. De Leo, O. Parcollet, G. Kotliar, and A. Georges, *cond-mat/0806.4383* (2008).
¹⁷ M. Takahashi, *J. Phys. C: Solid State Phys.* **10**, 1289 (1977).
¹⁸ A. H. MacDonald, S. Girvin, and D. Yoshioka, *Phys. Rev. B* **37**, 9753 (1988).
¹⁹ T. Yoshida, X. J. Zhou, K. Tanaka, W. L. Yang, Z. Hussain, Z.-X. Shen, A. Fujimori, S. Komiya, Y. Ando, H. Eisaki, et al., *cond-mat/0510608* (2005).
²⁰ A. Ino, C. Kim, T. Mizokawa, Z.-X. Shen, A. Fujimori, M. Takaba, K. Tamasaku, H. Eisaki, and S. Uchida, *J. Phys. Soc. Japan* **68**, 1496 (1999).
²¹ A. Ino, C. Kim, M. Nakamura, T. Yoshida, T. Mizokawa, A. Fujimori, Z.-X. Shen, T. Kakeshita, H. Eisaki, and S. Uchida, *Phys. Rev. B* **65**, 094504 (2002).
²² D. Damascelli, Z. Hussain, and Z.-X. Shen, *Rev. Mod. Phys.* **75**, 473 (2003).
²³ H.-B. Schüttler and A. J. Fedro, *Phys. Rev. B* **45**, 7588 (1992).
²⁴ W. E. Pickett, *Rev. Mod. Phys.* **61**, 433 (1989).
²⁵ E. Pavarini, I. Dasgupta, T. Saha-Dasgupta, O. Jepsen, and O. K. Andersen, *Phys. Rev. Lett.* **87**, 047003 (2001).
²⁶ R. S. Markiewicz, S. Sahrakorpi, M. Lindroos, H. Lin, and A. Bansil, *Phys. Rev. B* **72**, 054519 (2005).
²⁷ C. Kim, P. J. White, Z.-X. Shen, T. Tohyama, Y. Shibata, S. Maekawa, B. O. Wells, Y. J. Kim, R. J. Birgeneau, and M. A. Kastner, *Phys. Rev. Lett.* **80**, 4245 (1998).
²⁸ P. W. Anderson, *Low Temperature Physics (Fizika Nizkikh Temperatur)* **32**, 282 (2006).
²⁹ A.-M. Tremblay, B. Kyung, and D. Sénéchal, *Low Temperature Physics (Fizika Nizkikh Temperatur)* **32**, 561 (2006).
³⁰ R. G. Melko and A. W. Sandvik, *Phys. Rev. E* **72**, 026702 (2005).
³¹ A. L. Chernyshev, D. Galanakis, P. Phillips, A. V. Rozhkov, and A.-M. S. Tremblay, *Phys. Rev. B* **70**, 235111 (2004).
³² A. B. Harris and R. V. Lange, *Phys. Rev.* **157**, 295 (1967).
³³ J.-Y. P. Delannoy, M. J. P. Gingras, P. C. W. Holdsworth, and A.-M. S. Tremblay, *Phys. Rev. B* **72**, 115114 (2005).
³⁴ A. W. Sandvik, S. Daul, R. R. P. Singh, and D. J. Scalapino, *Phys. Rev. Lett.* **89**, 247201 (2002).
³⁵ A. Läuchli, G. Schmid, and M. Troyer, *Phys. Rev. B* **67**, 100409 (2003).
³⁶ O. I. Motrunich, *Phys. Rev. B* **72**, 045105 (2005).
³⁷ M. Hermele, M. P. A. Fisher, and L. Balents, *Phys. Rev. B* **69**, 064404 (2004).
³⁸ A. H. Castro Neto, P. Pujol, and E. Fradkin, *Phys. Rev. B* **74**, 024302 (2006).
³⁹ P. W. Leung, B. O. Wells, and R. J. Gooding, *Phys. Rev. B* **56**, 6320 (1997).
⁴⁰ T. Tohyama and S. Maekawa, *Supercond. Sci. Technol.* **13**, R17 (2000).
⁴¹ O. K. Andersen, A. I. Liechtenstein, O. Jepsen, and F. Paulsen, *J. Phys. Chem. Solids* **56**, 1573 (1995).
⁴² D. Sénéchal and A.-M. S. Tremblay, *Phys. Rev. Lett.* **92**, 126401 (2004).
⁴³ J.-I. Igarashi, *Phys. Rev. B* **46**, 10763 (1992).
⁴⁴ Y. S. Lee, R. J. Birgeneau, M. A. Kastner, E. Y., S. Wakimoto, K. Yamada, R. W. Erwin, S.-H. Lee, and G. Shirane, *Phys. Rev. B* **60**, 3643 (1999).
⁴⁵ A. W. Sandvik and R. R. P. Singh, *Phys. Rev. Lett.* **86**, 528 (2001).
⁴⁶ W. Zheng, R. R. P. Singh, J. Oitmaa, O. P. Sushov, and C. Hamer, *Phys. Rev. B* **72**, 033107 (2005).
⁴⁷ A. M. Toader, J. P. Goff, M. Roger, N. Shannon, J. R. Stewart, and M. M. Enderle, *Phys. Rev. Lett.* **94**, 197202 (2005).
⁴⁸ L. Raymond, G. Albinet, and A.-M. S. Tremblay, *Phys. Rev. Lett.* **97**, 049701 (2006).
⁴⁹ S. Notbohm, P. Ribeiro, B. Lake, D. A. Tennant, K. P. Schmidt, G. S. Uhrig, C. Hess, R. Klingeler, G. Behr, B. Buchner, et al., *Phys. Rev. Lett.* **98**, 027403 (2007).
⁵⁰ A. M. Toader, J. P. Goff, M. Roger, N. Shannon, J. R. Stewart, and M. M. Enderle, *Phys. Rev. Lett.* **97**, 049702 (2006).

- ⁵¹ In the notation of Dirac, where the coupling constants are defined as coefficients of spin permutation operators, the term that corresponds to the permutation of four spins does not contribute to leading order in $1/S$. (See Ref. [47]).
- ⁵² When the coupling constant for four spin permutations is different from zero, comparisons with high temperature neutron scattering experiments suggest better agreement than when a pure second-neighbor ferromagnetic interaction is added phenomenologically without the four spin permutation term. (See Refs. [47,48,50]).
- ⁵³ A. Singh and P. Goswami, Phys. Rev. B **66**, 092402 (2002).
- ⁵⁴ N. M. R. Peres and M. A. N. Araújo, Phys. Rev. B **65**, 132404 (2002).
- ⁵⁵ A. Gagné-Lebrun and A.-M. Tremblay, *Proceedings of the 17th annual international symposium on High Performance Computing Systems and Applications and the OSCAR Symposium*, Ed. D. Sénéchal, NRC-CNRC Research Press, Ottawa p. 71 (2003).
- ⁵⁶ M. Vekic and S. R. White, Phys. Rev. B **47**, 1160 (1993).
- ⁵⁷ A. H. Nevidomskyy, C. Scheiber, D. Sénéchal, and A.-M. Tremblay, Phys. Rev. B (in press) (2008).
- ⁵⁸ B. Kyung and A.-M. Tremblay, Phys. Rev. Lett. **97**, 046402 (2006).
- ⁵⁹ J. R. Schrieffer, X. G. Wen, and S. C. Zhang, Phys. Rev. B **39**, 11663 (1989).
- ⁶⁰ C. Kittel, Quantum Theory of Solids (John Wiley Sons, Inc., New York, 1963).
- ⁶¹ T. Holstein and H. Primakoff, Phys. Rev. **58**, 1098 (1940).
- ⁶² Y.-Q. Li and U. Eckern, Phys. Rev. B **62**, 15493 (2000).
- ⁶³ S. A. Kivelson, I. P. Bindloss, E. Fradkin, V. Oganesyan, J. M. Tranquada, A. Kapitulnik, and C. Howald, Rev. Mod. Phys. **75**, 1201 (2003).
- ⁶⁴ A. Abragam and B. Bleaney, Electron Paramagnetic Resonance of Transition Ions (Clarendon, Oxford, 1970).
- ⁶⁵ M. Gross, E. Sánchez-Velasco, and E. Siggia, Phys. Rev. B **39**, 2484 (1989).
- ⁶⁶ K. J. Runge, Phys. Rev. B **45**, 7229 (1992).
- ⁶⁷ We remark that a spin-only Hamiltonian can also be obtained for the three-band model. (See Refs. [online-citeRoger:1989,Hartmann:2002]).
- ⁶⁸ E. Müller-Hartmann and A. Reischl, Eur. Phys. J. B **28**, 173 (2002).
- ⁶⁹ B. Kyung and A.-M. Tremblay, (unpublished) (2008).
- ⁷⁰ B. Kyung, S. S. Kancharla, D. Senechal, A.-M. S. Tremblay, M. Civelli, and G. Kotliar, Physical Review B **73**, 165114 (pages 6) (2006), URL <http://link.aps.org/abstract/PRB/v73/e165114>.
- ⁷¹ B. Kyung, J. Landry, D. Poulin, and A.-M. Tremblay, Phys. Rev. Lett. **90**, 099702 (2003).
- ⁷² T. Paiva, R. T. Scalettar, C. Huscroft, and A. K. McMahhan, Phys. Rev. B **63**, 125116 (2001).
- ⁷³ A. W. Sandvik, Phys. Rev. B **66**, 024418 (2002).
- ⁷⁴ O. P. Vajk, P. K. Mang, M. Greven, P. M. Gehring, and J. W. Lynn, Science **295**, 1691 (2002).
- ⁷⁵ A. R. Mucciolo, A. H. Castro Neto, and C. Chamon, Phys. Rev. B **69**, 214424 (2004).
- ⁷⁶ J.-Y. P. Delannoy, M. J. P. Gingras, P. C. W. Holdsworth, and A.-M. S. Tremblay, to be submitted (2007).
- ⁷⁷ Proof
- $$[T_1, M_H^\dagger] = -\frac{t}{2N} \sum_{i,j,k,\sigma,\sigma'} \left[n_{i\bar{\sigma}} c_{i\sigma}^\dagger c_{j\sigma} h_{j\bar{\sigma}}, \hat{\sigma}_{\sigma,\sigma'}^z n_{k,\sigma'} \right] (-1)^k,$$
- $$[T_1, M_H^\dagger] = -\frac{t}{2N} \sum_{i,j,k,\sigma,\sigma'} n_{i\bar{\sigma}} \left\{ \left[c_{i\sigma}^\dagger, n_{k,\sigma'} \right] c_{j\sigma} + c_{i\sigma}^\dagger \left[c_{j\sigma}, n_{k,\sigma'} \right] \right\} \times h_{j\bar{\sigma}} \hat{\sigma}_{\sigma,\sigma'}^z (-1)^k,$$
- hence,
- $$[T_1, M_H^\dagger] = -\frac{t}{2N} \sum_{i,j,\sigma} n_{i\bar{\sigma}} c_{i\sigma}^\dagger c_{j\sigma} h_{j\bar{\sigma}} \left(-(-1)^i + (-1)^j \right) \hat{\sigma}_{\sigma,\sigma}^z.$$
- Since $(-1)^i = -(-1)^j$ for nearest neighbors, we get the final result and can generalize it for T_{-1} and T_0 .
- ⁷⁸ Proof: Same calculation than in Eq. (48,49,50), but for second or third nearest neighbors, $(-1)^i = (-1)^j$.